DNA NANOTECHNOLOGY: DEVELOPING AND ANALYZING A NEW TOOL FOR SENSING ALLERGENS

A THESIS SUBMITTED TO THE FACULTY OF

UNIVERSITY OF MINNESOTA

BY

ANA PAULA BRUMANN CLEMENTE

IN PARTIAL FULFILLMENT OF THE REQUIREMENTS

FOR THE DEGREE OF MASTER OF SCIENCE

DR. THEODORE P. LABUZA

June, 2016

Acknowledgements

First, I would like to thank my advisor Dr. Ted Labuza, without whom this accomplishment would not be possible. Ted, thank you for give me this opportunity and share with me a little of your vast knowledge not just in Food Science but in life. Your way of conducting work gave me, even more, passion about our field and showed me that is possible to make a difference.

I would like also to profoundly thank Dr. Efrosini Kokkoli. Efie, thank you very much for helping me conduct this work. You showed me how passionate someone can be about their work, that is very inspiring for someone who is about to start their career.

Also thank you Dr. Tonya Schoenfuss for being part of this thesis committee. Tonya, you were one of the first professors that I got to know in our department you showed me how to get excited about work and your career is an inspiration to me.

A special thank you to Dr. Huihui Kuang for all the help with the lab work.

I also would like to thank my lab colleagues Luna and Ben. Luna, you are a great friend always helping in circumstance and you helped me to follow through. Ben thank you for always sharing laughs, knowledge and sometimes even frustrations. I feel very blessed and accomplished for have encountered so

many wonderful people during my time in the Department of Food Science and Nutrition.

Thank you CAPES (Coordenação de Aperfeiçoamento de Pessoal de Nível Superior), for the scholarship provided through the Brazil Scientific Mobility Program.

This work was supported through a MnDRIVE grant from the University of Minnesota.

Dedication

I dedicated this thesis to my family. Without them, nothing of these would be possible. On the most caring and lovable way supported me throughout the journey the brought me to this point of my life. Thank you so much, Bete and Rapha, you are the most important part of me.

Abstract

Allergens are a major problem especially concerning public health and economy. There are more than 150 foods that can initiate allergic reactions, these reactions can elicit a mild response or a dangerous life threatening condition and in some extreme cases death. Milk and milk ingredients are one of the 8 foods that are responsible for about 90% of all food related allergic reactions. Food containing undeclared allergens in the label are misbranded and adulterated, and in accordance with the FSMA law must be recalled. It is estimated that the food industry can spend up to $10 millions dollars in direct costs from a recall.

It was hypothesized that aptamer-amphiphile, a synthesis product from ssDNA aptamer and a hydrocarbon tale, in conjunction with liquid-crystal could be used as a sensor for detection of β-lactoglobulin, an allergenic whey protein. The sensor was based on the self-alignment properties of liquid crystals based on the environment that it is exposed and on the capabilities of DNA aptamers to specific binding to targets.

Results of this work showed that the aptamer-amphiphile of choice, amphiphile synthesized without a spacer between the DNA head group and the hydrocabon tail, had a great affinity to target, $K_d = 45 \pm 1.68$ nM. In addition to it, it was possible to demonstrate that the interaction of the aptamer-amphiphile with

the target protein, β-lactoglobulin, using the sensor assembly resulted in images that can be easily identified under the polarizing microscope, sensor exposed to the aptamer-amphiphile alone gave a black image, once the protein was introduced the image was bright.

Furthermore, the sensor developed has a limit of detection of 18.4ng of β-lactoglobulin. It was also able to selectively identify the target protein, since when aptamer-amphiphile supported on the sensor was exposed to a random protein the image did not change as it did with β-lactoglobulin. In conclusion, this sensor developed proves the concept that aptamer-amphiphile and the liquid crystal can potentially be used as a sensor technique in food plants to detect allergens in food contact surfaces.

Table of Contents

List of Tables

List of Figures

1. Introduction

1.1 Food allergy overview

An allergy is an immune system reaction that occurs when the body identifies a usually harmless compound, specifically a protein, as harmful. This triggers the production of immunoglobulin E (IgE), an antibody for the protein consumed. If a second exposure to that protein occurs, a binding reaction between the IgE and the allergenic food compound occurs and the body elicits a variety of responses, from mild reactions to dangerous life threatening conditions and in some cases death (National Institute of Allergy and Infectious Diseases 2012). According to the Food Allergy and Anaphylaxis Network, FAAN, (currently merged into Food Allergy Research & Education, FARE), food allergies account for about 300,000 emergency room visits every year and about 150 to 200 deaths every year (FDA 2009).

There are more than 150 foods that can initiate allergic reactions but 8 of them are responsible for more than 90% of the total allergic reactions, those foods are: milk (and milk ingredients), shellfish, eggs, fish, tree nuts (e.g. pistachios, almonds, walnuts), peanuts, wheat and soybeans (Figure 1) (Center for Food Safety and Applied Nutrition 2016). Among those foods some of them affect a larger section of the population than others, milk and its ingredients are the number one in cases among young children and shellfish is the most

prevalent among adults (Sampson 2004).

Figure 1 Illustrative representation of the big eight food allergens.

In 2007 there were about 9 million adults and 3 million children in the United States with some sort of food allergy, those numbers fluctuate but as a whole they are increasing (Figure 2). In accordance with the Center for Disease Control and Prevention, there was an 18% increase on food allergies from 1997 to 2007, for the number of children, 18 years of age or younger. In the case of children, those affected by allergies are more likely to develop other health issues such as asthma and nonfood related allergies (Branum and Lukacs 2008).

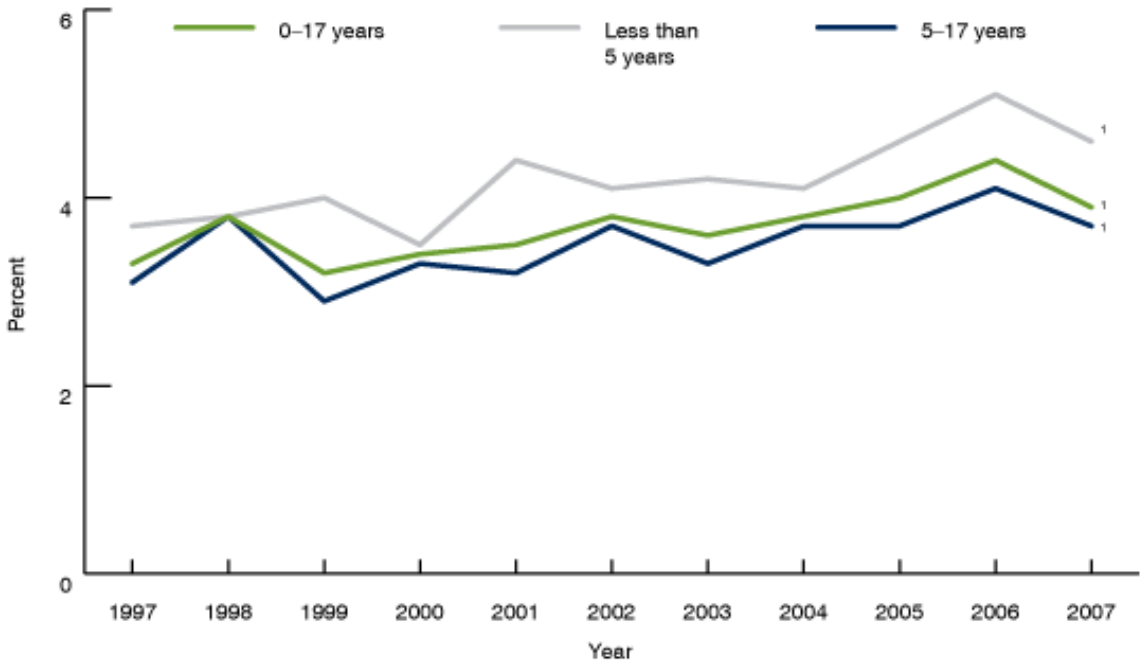

Figure 2 Percentage of children, under 18 years old, that presented some sort of food allergy. Source: (Branum and Lukacs 2008).

To further aggravate the problem there is no cure for food allergies, the FDA recommends that consumers avoid the food items that contains the specific allergenic protein that triggers the reactions. Keeping this recommendation as a priority, the agency is enforcing the Food Allergen Labeling and Consumer Protection Act 2004 (FALCPA) aims to create mechanisms to ensure that the product label matches the product content. The act requires that food containing any proteins derived from the eight major food allergens must be clearly stated on the label. Although FALCPA recognizes the allergen intentionally introduced in the food product, it does not draw attention to any allergenic ingredient accidentally introduced by cross-contact (contamination), the unintentional

contact of the food product with residual amounts of allergenic proteins on equipment surfaces or from aerosols (FDA 2009).

The Food Safety and Modernization Act, signed into law by President Obama in January 2011, has a dedicated section, Sec. 112, to food allergy and anaphylaxis management that targets education programs and schools. The law requires a preventive approach and expects those establishments in conjunction with state authorities create a voluntary plan to manage the risks in regards to allergens and anaphylaxis(Center for Food Safety and Applied Nutrition 2016a).

1.2 Food Allergies and the Economy

In addition to the health concerns, foods containing unlabeled allergens on the food package are appointed as being the number one cause of food recall in the United States. The Food Safety Magazine showed that between July and September 2015, more than 50% of all food recalls issued by U.S. Food and Drug Administration, U.S. Department of Agriculture USDA, U.S. Centers for Disease Control and Prevention (CDC), and the Canadian Food Inspection Agency were due to undeclared food allergens. Milk, the number one cause of recalls, was responsible for 18% of all the 122 recalls in that period of time (Maberry 2015). The ExpertRecall company also indicated that in a 1 year period between 2010 and 2011, undeclared food allergens were more prevalent than

any other food recall issued by FDA in that same period (Figure 3) (ExpertRECALL 2011).

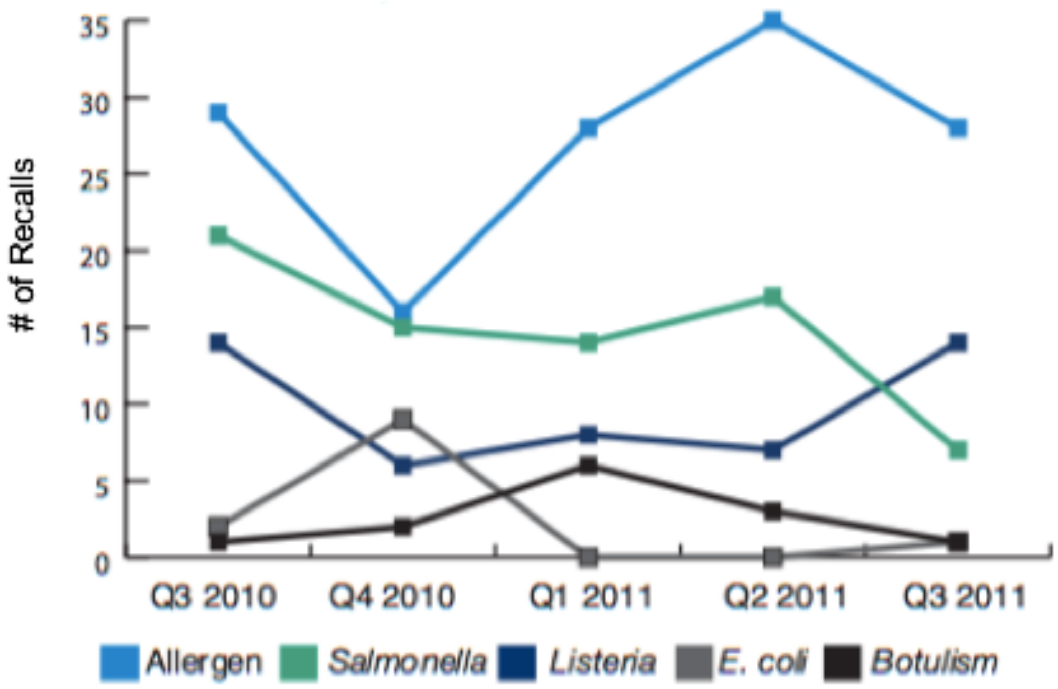

Figure 3 The number of food safety based recalls during the third quarter of 2010 until the third quarter of 2011. Source: (ExpertRECALL 2011)

A mandatory recall procedure is initiated once an undeclared allergen is detected, based upon the Food and Drug and Cosmetic Act and FSMA. Title 21 chapter 1 of this act mandates that food products with an untruthful label is misbranded and shall not be introduced, shipped, delivered or sold between interstate or US territory regions. Still within this act, Chapter 9, subchapter IV, section 342, defines adulterated food as “If it bears or contains any poisonous or deleterious substances which may render it injurious to health;”. (*21 USC Ch. 1:*

Adulterated or Misbranded Foods or Drugs From Title 21- Food and Drugs 1906; *21 USC 342: Adulterated Food From Tittle 21- Food and Drugs* 2016). As a result of these laws, foods containing undeclared allergens are considered adulterated and most likely misbranded and should be recalled.

Some independent insurance companies such as Tyco Integrated Security and Swiss Re performed studies to evaluate the real cost of a recall for the affected industry. Some of their finds are that food recalls cannot be evaluated just by the direct cost of the recall, but also the sales losses and brand damage. Considering dollar amounts Tyco concludes that on average, a recall for a food company can cost up to $10 million dollars in direct costs. In addition to the company costs, government costs in regard to public health needs to be considered as well, Swiss Re published in 2013 that food contamination costs the U.S health authorities more than $15 million (Tyco Integrated Security 2012; Swiss Re 2015).

1.3 Allergen Management

As previously mentioned, food containing undeclared allergens are considered adulterated as well as misbranded so it is crucial for the food industry to implement an effective allergens prevention programs under FSMA regulations. Some industries have been using advisory labels that state that the food product may contain a certain allergen, for example “ produced in a plant

that also produces peanuts", FDA under FALCPA does not endorse this use and believes that labels should be truthful not misleading (Center for Food Safety and Applied Nutrition 2006). To be lawful companies need an effective on or off line testing system that will provide legitimate information about the allergen presence of their food products. Some foods are known to be allergenic, others can become allergenic due to (1) cross-contamination, (2) the food was packaged in a box with the wrong ingredient statement on, (3) an ingredient supplier was not diligent about their product and did not indicate the use of an allergen in their certificate of analysis (COA).

The major test that is used to detect allergens in foods is the Enzyme-Linked Immunosorbent Assay (ELISA), which uses enzymes and a colorimetric reagent to measure the quantity of a specific analyte, either the antigen or the antibody, in solution. ELISA is a method that can provide a limit of detection in the parts per million range, it can be very selective and sensitive(Alvarez and Boye 2012). Whereas the method has its advantages it also has some limitations such as variable results if different antibodies are used, the calibrant used can also influence the final result, it is highly time-consuming and requires a trained analyst to perform the test (Immer and Lacorn 2015).

1.4 Research Needs

It has been noticed that the number of people with food allergies is increasing and the law is getting stricter towards allergens management. The food industry will need to be more diligent about allergen testing using a method that can tackle mainly the cross contamination problem.

1.5 Hypotheses and Objectives

The null hypotheses are:

1. Aptamers will not be able to detect proteins.
2. Aptamer-amphiphiles will not have affinity to β-lactoglobulin.
3. Liquid crystal cannot be used as a sensor.

The research objectives were:

1. Identify an aptamer that can target β-lactoglobulin with good binding constant.
2. Synthesize an aptamer-amphiphile that has binding affinity towards β-lactoglobulin.
3. Utilize liquid-crystal in conjunction with aptamer-amphiphile to develop a sensor for β-lactoglobulin.

2. Literature review

2.1 Beta-lactolgobulin (β-LG)

2.1.1 Beta-lactolgobulin properties

Cow's milk is on average, composed of 3% protein. There are two major types of proteins, the caseins and the whey proteins, however there are some other proteins in milk that cannot be classified as either, a small amount of the total. About 80% of all milk protein is composed of caseins. Whey protein corresponds to about 18% of all milk protein. Whey proteins, in general, are those that cannot be coagulated by acid at room temperature. However, if heated at a pH below 6.5 they will aggregate and become insoluble. Whey is constituted of four major proteins, β-lactoglobulin, α-lactalbumins, bovine serum albumin and immunoglobulins (Table 1) (Goff and Hill 1992; Walstra et al. 2006).

Table 1 Whey proteins (including common abbreviations) and its composition in skim milk (g/L). Adapted from (Farrell et al. 2004).

Protein	Composition in skim milk (g/L)
β-Lactoglobulin (β-LG)	2-4
α-lactalbumins (α-LA)	0.6-1.7
Serum albumins	0.4
Immunoglobulins	0.45-0.75

β-lactoglobulin is the major whey component, about 51% of the total cow's milk whey protein. β-lactoglobulin is a relatively small globular protein that has a

molecular weight of 18.28 kDa. The secondary structure of this protein is composed of α-helix and β-structure, at the milk pH of around 6.5, the protein is naturally present as a dimer linked by non-covalent interactions. β-LG is the prevalent whey protein in a variety of ruminant's milk such as: cow, goat, and sheep. Some other mammals such as dolphins, kangaroos and manatees also produce β-LG. However, β-LG does not occur in human milk. (Goff and Hill 1992; Walstra et al. 2006).

Some other physicochemical characteristics of β-LG includes a tolerance to enzymatic proteolytic activity, enzyme might not be able to coagulate the protein. The neutrally charged state occurs at pH 5.1, its isoelectric point. The salt content presents a greater impact on solubility, an increase in salt content will increase solubility in the same solvent and pH. The denaturation process will occur due to alkalinity, temperature, pressure, solvent and presence of ions, for example if heated to 90°C for about 10 min, it will denature. Alkalinity also poses as an important factor for denaturation, above pH 8 it is already possible to verify changes in the structure (McSweeney and Fox 2009).

2.1.2 Beta-lactoglobulin allergenicity

When considering allergens, it is known that the whole protein is not responsible for the allergic reaction, only the epitope region, triggers the immune system. The epitope is a region on the surface of the allergenic compound that

interacts with IgE antibodies. Among food epitopes, there are two classes, those called the T-cell epitopes that have a linear amino acid sequence and the B-cell epitopes that are conformational epitopes. Milk allergen regions were identified as being linear B-cell epitopes, most likely due to conformational changes during processing steps (Chen and Gao 2012).

β-lactoglobulin is identified as being the more allergenic protein among all milk proteins, other milk proteins can also cause allergic reactions such as α-lactoalbumin, casein and lactoferrin. Due to its physical-chemical properties, resistance to pepsin and acid resistance, β-LG can goes through the digestion system reaching the intestine and triggering allergic reactions (Luo and Bu 2012). Brownlow *et al.*(1997) classified β-lactoglobulin as part of the lipocalin family due to its structural similarity, eight antiparallel β strands composing what is a call a β barrel. This structural classification corroborates with β-LG allergenic potential since all lipocalins present a high allergenic potential (Luo and Bu 2012).

Some attempts have been made to reduce allergic potential using heat treatment, Ehn *et.al.* (2004) observed a small but significant change in the antigenicity capabilities with 15 minutes exposure at 74°C. Even though this heat treatment was able to reduce the allergenic potential it was not able to eliminate all the epitopes of the protein. Another study used a temperature treatment that exposed the protein to temperatures above 90°C, but still there was no significant deletion of allergenic response (Luo and Bu 2012). In addition, Williams and

Davis (1998) observed that when denatured β-LG developed, at least, one new allergenic epitope region.

It is assumed that the array of symptoms that an allergic reaction can cause varies due to the level of exposure to the allergenic protein. There are other factors that play an important role in the symptoms such as level of stress of the subjected person, overall health, some medications, etc. It is evident that person to person variations will occur so evaluation of allergens exposure level/effect ratio to obtain a universal number is challenging and even ethically questionable (Taylor et al. 2009).

To evaluate the effectiveness of allergenic reactions, according to Taylor et al (2013), a threshold level should be defined as " the highest amount of the allergenic food that will not cause a reaction in individuals who are allergic to that food". This definition could be called NOAEL (No Observed Adverse Effect Level), which can be evaluated per person or by a population average. In an attempt to evaluate allergenic effects, controlled clinical challenge tests such as the double-blind, placebo-controlled, food challenges (DBPCFCs) and the single-blind, place controlled food challenges (SBPCFCs) are tests that evaluate patient response after exposure to the suspected allergenic protein (Taylor et al. 2004).

These tests were used in attempts to evaluate the NOAEL levels for milk proteins. One study that tested 100 patients concludes that the NOAEL for that population was 2mg of the allergenic protein or 0.02mL of fluid milk. Another

study that tested 31 patients obtained an NOAEL of 15mg of the allergenic protein or 0.5mL of fluid milk. Observing these NOAEL numbers, the conclusion is that no consensus number were obtained. Furthermore, it is important to highlight that these tests were performed using fluid milk and since milk allergenicity is due to several epitope regions in different proteins it is impossible to say which protein caused the reaction observed (Taylor et al. 2004).

Testing a defined number of people and them extrapolating to the whole population is suspect as we don't know the range of response of those subject to the allergen epitope. Even though those NOAEL numbers represent just some studies it is possible to say that overall no concrete affirmation can be made about the minimum level that causes an allergic response (Taylor et al. 2004).

2.2 Aptamers

2.2.1 What are aptamers?

An aptamer has its origin around 1990 when two separate research group were investigating RNA properties. Tuerk and Gold (1990) were investigating the interaction of bacteriophage polymerase and the ribosome binding site of mRNA at University of Colorado when they introduced the Systemic Evolution of Ligands by Exponential Enrichment (SELEX) process to select specific nucleotide molecules for a designated target. At about the same time, Ellington and Szostak (1990) were also investigating how RNA fragments can be selected

for specific binding of a target, the selected fragment was named Aptamers, the word originated from the Latin '*aptus'* that means to fit.

Aptamers were then defined as being single-stranded oligonucleotide ligands with specific binding power to a selected target. This can range from small oligonucleotide to larger more complex oligonucleotides structures which fold into a specific tertiary structure (Famulok et al. 2000). The SELEX process developed in 1990 by the researchers in Colorado and in Massachusetts is still the one used nowadays, with improvements and variations, to select oligonucleotides for specific targets.

SELEX is an in vitro process that involves selection and polymerase chain reactions (PCR), it consists of four basics steps, starting with a randomized oligonucleotides sequence being incubated with the target under specific conditions to promote binding. This is followed by a key step that will subtract from the oligonucleotide mixture those that do not bind to the target. The remaining oligonucleotide-target complex needs to be dissociated for the last step that involves the amplifications by PCR of the bind oligonucleotide sequences to obtain the aptamers. SELEX is usually performed in what is called a selection cycle where the four steps are repeated until aptamers that have a high affinity and specificity to target are selected (Aquino-Jarquin and Toscano-Garibay 2011).

One notorious method among the improved SELEX methods is the CE-SELEX which uses capillary electrophoresis (CE) to facilitate the selection cycles. A common SELEX procedure can take up to 15 cycles, while using CE can facilitate and speed the process, sometimes only using two full cycles. In addition to the time advantages, CE-SELEX is performed in solution which is an improvement from the original SELEX process where the target molecule was immobilized on a column where the DNA pool will be eluted through (Mendonsa and Bowser 2004).

Aptamers are typically small oligonucleotides sequences 15-45 bases, 5-15kDa, with high-affinity reaching the sub-nanomolar magnitude with capabilities to differentiate closely related targets (Aquino-Jarquin and Toscano-Garibay 2011). McGown and Rehder (2001) used these capabilities to differentiate two variants of β-lactoglobulin, LgA and LgB, using a 4-plane g-quadruplex former aptamer sequence , 5'-GGGGTTGGGGTGTGGGGTTGGGG-3', as the stationary phase in open-tubular capillary electrochromatography (OTCEC). This same sequence was used throughout this work as the targeting aptamer for β-lactoglobulin.

G-quadruplex is one of a variety of secondary structures formed by DNA fragments. In this case two or more planar G-quarters structures (Figure 4), composed of four guanines interacting through H-bonds, are stacked. These structures started to be explored when Gellert *et. al.* (1962) elucidated that the

potential for guanylic acid to form gels in the millimolar range is due to this special tri-dimensional assembly, those gels were first observed by Bang in 1910 (Bryan and Baumann 2010).

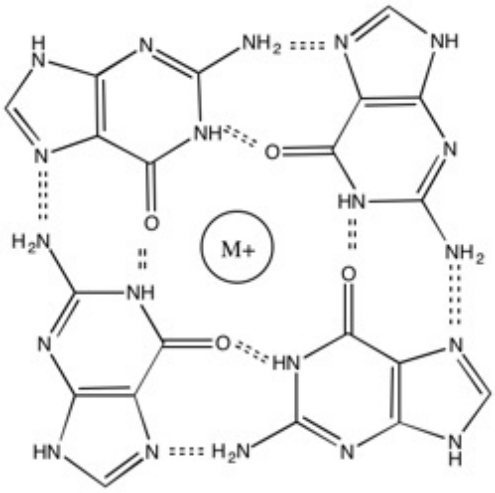

Figure 4 Illustrative representation of the G-quarter structure.

G-quarter structures are stabilized by cation molecules embedded in the center of the four guanine molecules, represented by M+ in Figure 4, these cations will largely influence the stability of the overall structure. Another interesting trait of these structures is the ability to form inter or intramolecular G-quadruplex structure. There are three different possible orientations for G-quadruplex, parallel, antiparallel and hybrid (Figure 5). These differ based upon how the guanine molecules interact and it is modulated by the DNA sequence and by the environment it is exposed to (Bryan and Baumann 2010).

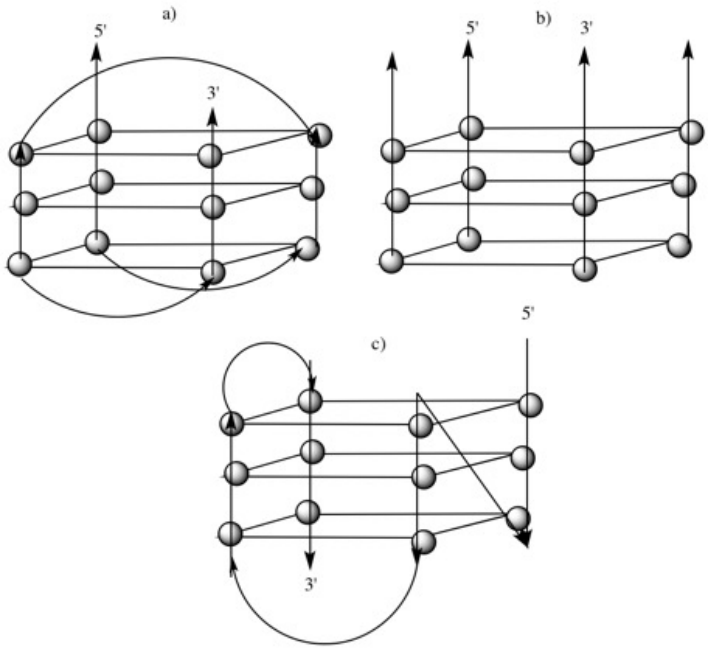

Figure 5 Schematic representation of the possible G-quadruplex assemblies. a) Antiparallel, b) parallel, and c) hybrid

As previously mentioned, aptamers fold in specific tridimensional structures. To evaluate these structures, a technique called Circular Dichroism Spectroscopy (CD) is used, this technique uses polarized light to evaluate molecular conformation. In biochemistry analysis, CD is largely used to differentiate between an α helix, β sheet, and a random coil polypeptide chain so as to evaluate DNA conformation. This technique uses a parameter called ellipticity what describes the absorption difference between the right- and left-circularly polarized light (Woody 1995).

Among the three different guanine quadruplexes, two of them can be differentiated by circular dichroism. The parallel G-quadruplex spectrum will have

two strong positive peaks, one around 210 nm and another one around 260 nm. For antiparallel there are two strong positive bands, 210 nm and 290 nm, and also a negative band around 260 nm (Kypr et al. 2009).

2.2.2 Aptamer advantages

The comparison between aptamers and antibodies as to binding to an allergenic epitope is inevitable since both substances are used to selectively target a desired compound, and consequently both can be used in detecting techniques. Since the SELEX process was developed, aptamers are gaining more attention and are being recognized for being a more flexible substance with some advantages in comparison to antibodies, Table 2. With more technological improvement there is an urge to be able to sense and detect any substance of desire, aptamers are playing an important role in trying to fulfill this need (Jayasena 1999).

Table 2 Summary of aptamer advantages in comparison to antibodies (Toh et al. 2015).

	Aptamers	***Antibodies***
Selection type and price	In vitro, less expensive	In vivo, more expensive
Molecule Size	Usually small	Large
Target	Almost any molecule	High immunogenicity targets only
Resistance	Stable at room temperature and some mild temperature elevation	Denature at room temperature
Chemical Modification	Easily modified to the desired use	In vivo process make it challenging

The antibody selection process starts with a biological system, specifically an animal, this is the first disadvantage since the immune system response may fail to recognize the antigen. This recognition problem may happen if for example the desired antigen is a protein very similar to an endogenous protein of the animal. Also, antibody production problems may happen if the antigen is a toxin molecule to the immune system of the animal. Another downfall to antibodies is the batch to batch variations since the live organism will vary. (Luzi et al. 2003). For aptamers, on the other hand, the selection process is totally in vitro, SELEX utilized randomized synthetically produced oligonucleotides pool and select the desired aptamer using only analytical methods what gives good reproducibility and no inherit variability (Aquino-Jarquin and Toscano-Garibay 2011).

Another highly desirable characteristic of aptamer use is its thermal stability, i.e. having the ability to recover its original conformation after thermal denaturation. Antibodies, on the other hand, are large proteins that usually are irreversibly denatured by heat. As previously mentioned, specific aptamers are the result of an in vitro selection process that makes it possible to get a target sequence for any substance including selecting for specific part of this target by the aptamer. Antibodies are limited to formation as a response to immune system invasion. The size restrictions of antibodies makes it difficult for them to react to intracellular targets, those previously blocked areas can easily be reached by aptamers (Luzi et al. 2003).

Per definition aptamers are small DNA or RNA fragments what give them the advantage of being easily labeled or chemically modified. A modification that is widely used in aptamers is the addition of a fluorophore molecule for the application as an optical sensor. This modification can be done in a variety of ways, for example, a specific oligonucleotide can be conjugated to the fluorophore or an organic fluorophore molecule can be anchored in the 5’ end of the DNA sequence. Biotin is commonly used as a modifier for certain applications, usually, the aptamer is synthesized with a biotin molecule either on the 5’ or 3’end of the nucleotide. There are also cases where combinations of modifications are utilized such as, but not limited to, a fluorophore molecule on one end a biotin on the other end (Cho et al. 2009).

One of those modifications that is beginning to gain attention lately is the attachment of an hydrocarbon tale on the end of a single strained DNA aptamer, i.e. a ssDNA-amphiphiles. Briefly, these are compounds that have dual opposite affinity towards the solvent, one part of the molecule would be attracted to the solvent and the other part of the molecule would be repulsed by the solvent. These molecules carry a very interesting characteristic inherent to amphiphiles, the ability to self-assemble in to tridimensional nanostructures. Peptide-amphiphiles have been explored for a long time, with the use of peptides as the headgroup. Attaching an amphiphile provides a variety of possible applications, such as drug delivery and molecular diagnostics (Pearce 2014).

An ssDNA-amphiphile is a relatively new research topic in comparison to the peptide-amphiphile so the majority of the work that has been published about it involves its synthesis and development. Pearce et al. (2014) utilized a strategy previous employed to peptide-amphiphiles, varying the spacer utilized to attached the hydrophobic tail to the hydrophilic DNA headgroup. This modulates the self-assembly of ssDNA-amphiphiles. Using this approach, but this time for an specific aptamer-amphiphile, Waybrant et al. (2014) evaluated how the tail and several spacers would influence the binding affinity to the FKN-S2 aptamer to the cell surface protein fractalkine (CX3CL1). They were able to conclude that the addition of the tail reduces the binding affinity to the select target while different spacers can either improve or worsen the binding affinity.

2.2.3 Aptamers in food safety applications

In recent year concerns about food safety have risen within the general public. The CDC estimated in 2011 that every year, about 50 thousand people got sick, 130 thousand are hospitalized and 3 thousand die of foodborne disease (Centers for Disease Control and Prevention 2011). Those alarming statistics and the emergence of aptamers as a potential sensing molecule started in the past 5 years as a research focus where researchers are trying to identify aptamers that specific binding to pathogens, exogenous substances such as antibiotics, bioterror agents like ricin, pesticides, and others (Dong et al. 2014).

Bruno et al. (2010) developed a method to detect the *E.coli* strain 8739 using an aptamer in a fluorescence resonance energy transfer (FRET) biosensor. This method used fluorophore molecules on the aptamer and was able to detect as little as 30 live bacteria per ml of buffer, this was good but the FDA adulteration limit is one bacterium in 25 g or less. A conjoint research initiative from the Hitachi Chemical Research Center and the Department of Food Science at Purdue University (2010) was able to develop a biosensor for the most deadly foodborne pathogen *Listeria monocytogens.* A specific protein of the microorganism was selected as the target for the aptamer and the biosensor assembly used an anti-*Listeria* antibody designated aptamer and fiber-optic. The developed sensor presented with a high sensitivity with a limit of detection of 1 $x10^3$ CFU/mL in buffer, thus much higher than FDA 1 CFU/25 g adulterated level.

This study also did some testing in inoculated foods concluding that the method is capable of detection of the pathogen in foods, but in our consideration, not a method to replace the 1 CFU/ 25 g legal limit.

Another food that was subjected to a method based on aptamer was milk. Zhang et al. (2010) developed an aptamer sensor for the antibiotic tetracycline. This work employed glassy carbon (GC) electrodes. The method was proven to be sensitive and fast with a limit of detection of 1ng/mL and an analysis time of 5min. Two very important toxins that are of concern for food safety were the target in studies using aptamers as a capture material. Lamont et al. (2011) selected an aptamer that was applied in a Raman spectroscopy method for detection of ricin in liquid food, orange juice, apple juice, lemonade and 2%milk, with a limit of detection of 30 ng/mL. Overall this method outcompeted the commercially available ELISA one for ricin. Aflatoxins were also the subject of study, a chemiluminescence method was developed for aflatoxin B1 (AFB1) in corn, in this case, the aptamer was linked to an DNAzyme and the method had a limit of detection of 0.11 ng/mL.

When considering food safety, not only for foodborne pathogens and toxins, allergens can also be incorporated in this hunt for detection. Aptamers have been tested to be used for allergen detection in food matrices. Peanuts, which is part of the big 8 allergens list, was the target of a study by Trans et al. (2013) where the major allergenic protein in peanuts, Ara h 1, was used as the

target for the aptamer that was developed using CE-SELEX. This aptamer was employed in a home-built fiber optic surface plasmon resonance (FO-SPR) biosensor that successfully detected the presence of the protein either in buffer and also in a food matrix, i.e. candy bar.

Gluten is also another very important recognized allergen. Wheat allergy is in the big 8 group. A method using aptamers was developed by Amaya-González et al. (2015). This method targets α2-gliadin using magnetic beads as the carrier for the competitive assay between the biotinylated aptamer and the selected peptide of the gliadin. For the sensing technique, the method attached the aptamer labeled with streptavidin-peroxidase. The enzyme activity is then measured by chronoamperometry screen printed electrodes. This work tested the method on some food samples such as millet flour, quinoa, maize flour, rice flour and others. The authors were able to show that the method developed had a limit of detection of 0.5 ppm.

2.2.4 Binding Study

When considering aptamers for a certain application, it usually is stated that the aptamer needs to have a good affinity for the target. Even the aptamer definition states this that aptamers are a single strained oligonucleotide that binds with high affinity to a target. So to access binding there are some methods such as gas chromatography, capillary electrophoresis, HPLC, UV-Vis

absorption, surface plasmon resonance, modified ELISA procedure, and others (Jing, Meng and Bowser 2012). For the scope of this work, the techniques of capillary electrophoresis and modified ELISA were explored. Furthermore, when accessing aptamer-target binding the dissociation constant (K_d) is usually the variable utilized as a measure of binding. The lower the K_d value the more affinity the aptamer to the target.

Capillary electrophoresis (CE) is a technique that according to Jing, Meng, and Bowser (2012) separates analytes in free solution based on their size and charge. CE has some advantages such as high resolution, small sample volume, and analysis in free solution. Within capillary electrophoresis, there are some different methodologies that can be used, for example, affinity capillary electrophoresis (ACE), the frontal analysis (FA), vacancy peak (VP) and vacancy affinity capillary electrophoresis (VACE). Those methods differ in how binding parameters would be observed, for VP the peak area is extracted, for FA the plateau height and for ACE and VACE the change in mobility is the desired variable (Busch et al. 1997).

In this work a frontal analysis methodology was used, results on Appendix A. Frontal analysis is a method where the capillary is filled with buffer and followed by the sample injection. The sample contains an equilibrium of target and aptamer. For this method there are two important assumptions, one is that the target/aptamer complex will not dissociate and the free aptamer will have a

significantly different mobility than target/aptamer complex (Busch et al. 1997). Girardot et al. (2011) developed a continuous frontal analysis using microchip electrophoresis (FACMCE), to evaluate the binding between lysozyme and its aptamer. From which the theory was used as the basis for the method used in this work.

The FACMCE method developed uses a fluorescently labeled aptamer and bases all the measurements in the fluorescent signal difference and plateau height difference, between the free aptamer and the aptamer in the presence of the target. It also uses mathematical linearization to obtain the K_d, using an x reciprocal method. The following equation can be used to obtain the K_d.

$$\frac{r}{[L]} = \frac{n}{K_d} - \frac{r}{K_d} \quad (1)$$

In the equation (Eq.(1)) r is the mean numbers of aptamers bound to the target, [L] is the concentration of the aptamer and n is the number of binding sites. The authors plotted the fluorescent signal difference of free aptamer and aptamer with the target versus the aptamer concentration. From that curve the K_d will be slope and n will be the intercept/slope (Girardot et al. 2013).

The enzyme-linked immunosorbent assay, ELISA, is a technique that is based on the antigen-antibody binding relationship, usually one of the elements is labeled with an enzyme for quantification purposes. Currently, the method more frequently used is a solid phase method where one of the components is attached to the surface of a well, if the antibody is attached that is called the

sandwich format and if the antigen is bound to the well this will be called the competitive format (Figure 6) (Immer and Lacorn 2015).

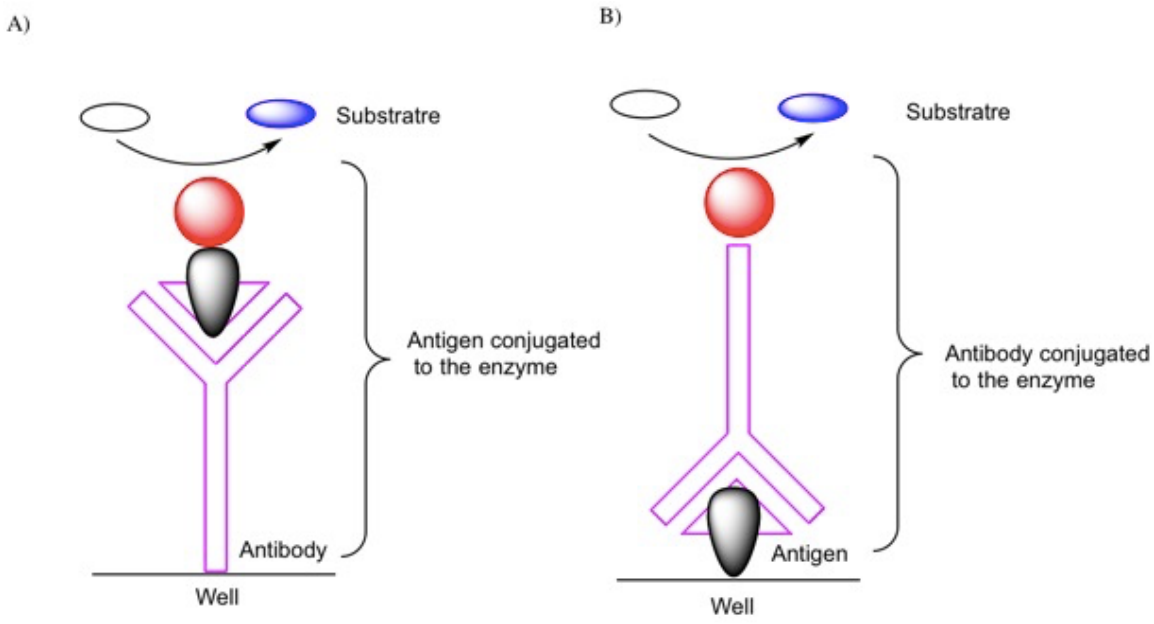

Figure 6 Illustrative representation of A) Sandwich ELISA and B) Competitive ELISA

With the known similarity between aptamers and antibody, some modified ELISA procedures are being developed where the antibody is substituted with an aptamer. New names are being used to identify those new methods such as ELASA- enzyme linked apta sorbent assay, ELAA-enzyme-linked aptamer assay, and ALISA-enzyme-linked-immobilized sorbent assay. Despite the different names, all of those new techniques, carry the advantages that aptamers have over antibodies. To standardize this, these new techniques are referred to as

ELASA throughout this work, where the A replaces the first I in ELISA (Toh et al. 2015).

The ELASA methods can be performed using the same strategies used for ELISA procedures such as: (1) immobilization of the aptamer on the capture surface; (2) direct ELASA that is characterized by the target being immobilized by using a biotinylated aptamer to bind the target; (3) indirect ELASA where in this case the target is immobilized and an antibody is bound to this target followed by an aptamer that has affinity to the antibody used; (4) sandwich ELASA where in this case, the aptamer or antibody is immobilized followed by the addition of the target and subsequently an enzyme-labeled aptamer or antibody is introduced. All of these methods use an enzyme substrate system to cause a reaction and give a signal emission that detected by some spectrographic mehtod (Toh et al. 2015).

To use ELASA for the dissociation constant determination a very common method used is the direct ELASA (Toh et al. 2015). Shroff et al (2012) developed a method using the basis for an indirect ELASA or ELISA since in this case it is used to evaluate the binding affinity of a peptide amphiphile to a protein. To evaluate the K_d, they designed a procedure where a constant amount of protein is immobilized in a 96-well plate and a biotinylated peptide-amphiphile is used as the binding molecule, bovine serum albumin (BSA) was used as the blocking agent and neutravidin-horseradish peroxidase (HRP) and 3,3',5,5'-

tetramethylbenzidine (TMB) was the enzyme-substrate of choice to give the signal.

The procedure was carried out by measuring the UV- Vis absorbance (450nm) and the obtained absorbance versus aptamer concentrations was fitted in a non-linear least-squares regression. The following equation was used to calculate the dissociation constant (Shroff et al. 2012):

$$\boldsymbol{B} = \frac{\boldsymbol{B_{max}}\ \boldsymbol{x}\ [\boldsymbol{A}]}{(\boldsymbol{K_d}+[\boldsymbol{A}])} \quad \textbf{(2)}$$

Where:

B= binding

B_{max}= saturated binding

[A]= aptamer concentration

All the math involved in the binding constant determination originates from chemical equilibriums theory and protein-protein interactions. Some assumptions are made to get the equation (Eq. (1)) such as the stoichiometry of the reaction is 1:1, the binding is reversible, no other chemical reactions is undergoing at the same time, and the aptamer concentration, [A], is much bigger than the K_d (Obenauer and Yaffe 2004). This procedure was used as the reference for the ELASA binding constant determination in this work.

2.3 Liquid Crystals (LC)

2.3.1 Definition and Properties

Liquid Crystal as the name indicates is a substance that presents a bivalent state of matter characteristic, intermediate between a liquid and a solid, it can flow as a liquid and form organized molecular arrays as solids. In general, organic molecules that present liquid crystallinity characteristics in the absence of a solvent are called thermotropic liquid crystals since their phase properties will be modulated by temperature (Lockwood et al. 2008). This structure possibility a variety of phases of liquid crystals, one of the most studied is the nematic phase liquid crystals (Figure 7), in this arrangement all the organic molecules within the crystal tend to be parallel organized but presenting no long range positional ordering (Jerome 1999).

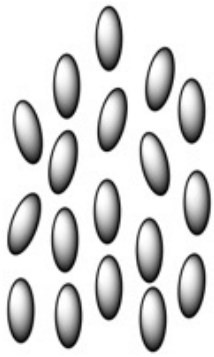

Figure 7 Illustrative representation of a nematic phase liquid crystal

Most of the work being developed in surface studies uses water-immiscible thermotropic LC in the nematic phase, these works take advantage of a unique characteristic of liquid crystals, the ability to easily be aligned with the contact surface (solid, vapor or immiscible liquid). The LC will organize in accordance with the chemistry and geometry of the surface. This is called anchoring of liquid crystals. A specific thermotropic nematic liquid crystal that is largely used in sensing techniques is the 4-*n*-pentyl-4'-cyanobiphenyl (5CB) (Figure 8) (Nazarenko and Nych 1999; Lockwood et al. 2008).

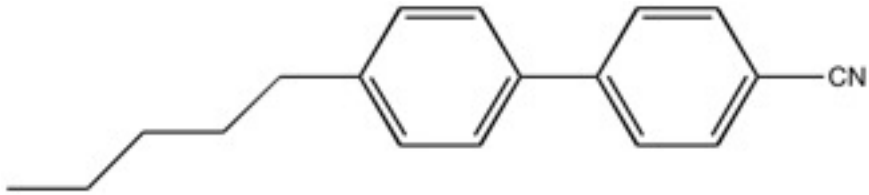

Figure 8 Chemical structure of the Liquid Crystal 5CB

Exposing the immiscible LC to water based solutions will cause the alignment of the liquid crystal. There are two interchangeable alignments largely explored in the application of LC as a sensor, planar anchoring, and homeotropic. In the planar anchoring, the molecules are parallel to the surface in the proximities of the solution. On the homeotropic alignment, the molecules are perpendicularly aligned with the interface. Associating polarized light microscopy and LC it is possible to design experiments to explore the LC characteristics obtaining images that reflect the different LC orientations (Lockwood et al. 2008).

2.3.2 Liquid crystal sensor applications

Exploring the anchoring and ordering properties of the LC, scientists are using several approaches to develop sensors using LC as the sensing tool. Brake and Abbott (2002a) developed an experimental system that allows for the observation of the transition from parallel to homeotropic, and vice-versa, using a polarizing microscope. Briefly, the simple system was comprised by copper grids supported on a glass slide filled with octadecyltrichlorosilane (OTS), that will give an homeotropic alignment layer. The liquid crystal, 5CB, is confined within the grid and the well contents can be exposed to several aqueous solutions containing variables amount of an amphiphle, in this case sodium dodecyl sulfate (SDS). The apparatus is then observed under the polarizing microscope in transmission mode and they conclude that when exposed to 0.0 mM SDS the image is bright indicating a parallel alignment, and in the presence of 2.2 mM SDS the image is dark indicating an homeotropic alignment (Figure 9). This same setup will be used in the experimental section of this thesis as the basis for the sensor that will be developed.

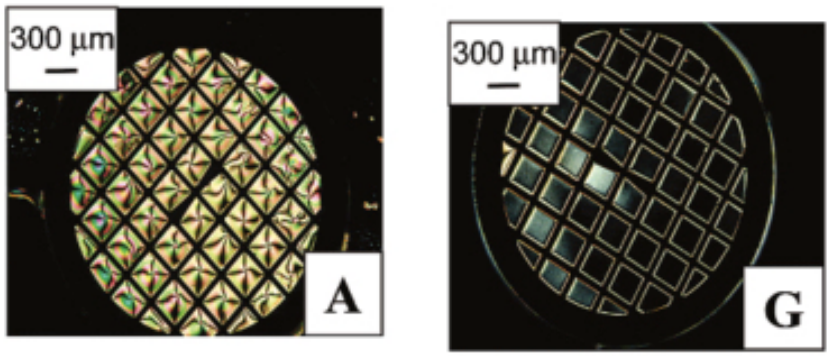

Figure 9 Images obtained by the different liquid crystal aligments. A- Exposed to water parallel alignments and G- Exposed to 2.2mM SDS hometropic alignment. Adapted from:(Brake and Abbott 2002a)

Another very interesting study using LC was done by McUmber et al. (2012), where a similar approach was used for the liquid crystal apparatus, LC confined within a grid and exposed to an alignment layer. In this study the LC alignment properties were used to differentiate single-stranded DNA from double-stranded-DNA. A surfactant was hybridized in the LC, and the interaction of the surfactant with the ssDNA promotes the LC reorientation. Noonan et al. (2013) also used DNA aptamers and surfactant-laden aqueous/liquid crystals but in their work, they were evaluating how target binding to aptamers would trigger LC reorientation. This work resulted in a sensor that was selective and sensitive, no response was obtained for analogous targets and the reorientation was observed in targets concentration in the same order as the dissociation constant.

Those are just some examples of LC versatility can be used as a sensing technique. Furthermore, associated with different kinds of molecules, it is

possible to obtain powerful tools that can be applied in the field. In this work a liquid crystal sensor associated with aptamer-amphiphiles will be used to detect β-lactoglobulin.

3. Materials and Methods

3.1 Circular Dichroism

3.1.1 Materials

Nuclease free-water (Integrated DNA Technologies, Coralville, IA), sodium chloride crystal (NaCl) (Macron Fine Chemicals, Center Valley, PA), magnesium chloride anhydrous 99%($MgCl_2$) (Alfa Aesar, Ward Hill, MA), potassium chloride granular (KCl) (Mallinckrodt Chemicals, Center Valley, PA), DNA aptamer 5'-GGG GTT GGG GTG TGG GGT TGG GG-3', DNA aptamer biotinylated modified 5'-/5Biosg/ GGG GTT GGG GTG TGG GGT TGG GG-3', DNA aptamer amine modifier 5'- GGG GTT GGG GTG TGG GGT TGG GG/3AmMO/ 3'(this sequence was used as the base for all the different aptamer-amphiphiles, the synthesis will be elucidated latter in this chapter, Table 3 represents all the synthesis performed) all purchased from Integrated DNA Technologies (Coralville, IA), 0.1 cm path length crystal cuvette, circular dichroism spectrometer Jasco J-815.

Table 3 Sequences and structures of the aptamer-amphiphiles synthesized and analyzed by CD.

Aptamer Sequence Aptamer-Amphiphile
5'- GGG GTT GGG GTG TGG GGT TGG GG/3AmMO/ 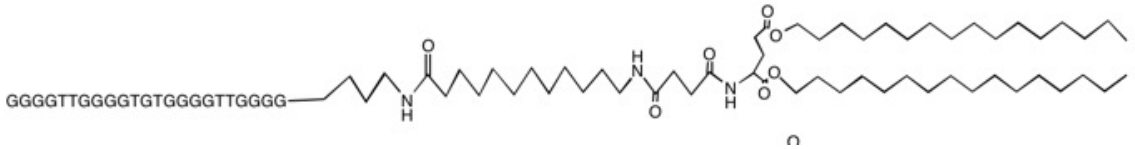   C12 Spacer Amphiphile (C12)
5'- /5Biosg/ GGG GTT GGG GTG TGG GGT TGG GG/3AmMO/    C12 Spacer Amphiphile Biotin (C12B)
5'- /5Biosg/ GGG GTT GGG GTG TGG GGT TGG GG/3AmMO/ 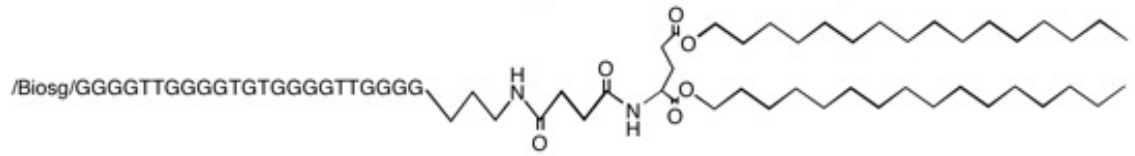   No Spacer Biotin Amphiphile (NoSPRB)
5'- /5Biosg/ GGG GTT GGG GTG TGG GGT TGG GG/3AmMO/ 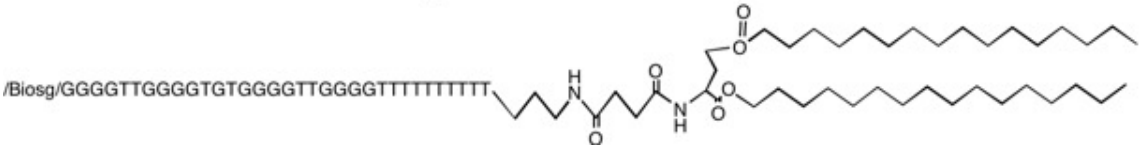   T10 Spacer Biotin Amphiphile (T10B)
5'- /5Biosg/ GGG GTT GGG GTG TGG GGT TGG GG/3AmMO/ 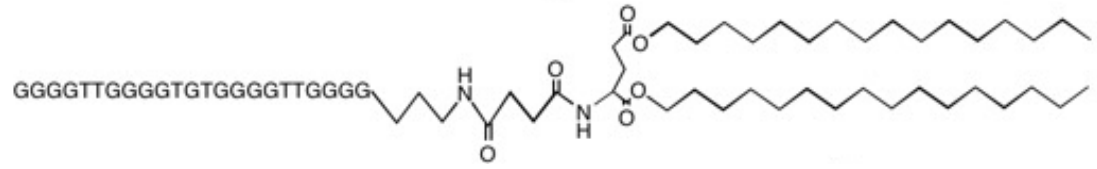   No Spacer Amphiphile (NoSPR)

3.1.2 Methods

For the DNA-aptamer, 10 μM solutions were made in three different electrolytes, 10 mM $MgCl_2$, 10mM NaCl, 10 mM KCl and in nuclease free water. For the biotinylated aptamer and all the aptamer-amphiphiles, the electrolyte of choice was 10 mM NaCl. The measurement was performed in the same way for all solutions. The solutions were transferred into a 0.1 cm path length cuvette and their CD spectra were obtained using a Jasco J-815 spectrometer. Three replicates were collected from 320-200 nm, with 1 mm increments at 50 nm/min read speed, subtracting the electrolytes spectra. The raw ellipticity data were averaged and converted to molar ellipticity (Θ), the data was smoothed with Matlab filter.

3.2 ELASA

3.2.1 Materials

Polystyrene 96-well EIA/RIA clear flat bottom plates (Corning, Pittston, PA), phosphate buffered saline (PBS) tablets (VWR, Radnor PA), Tween® 20 (Fisher Scientific, Hanover Park, IL), β-lactoglobulin (Davisco Foods International, Eden Prairie, MN), α-lactalbumin (Davisco Foods International, Eden Prairie, MN), Ovalbumin (Fisher Scientific, Hanover Park, IL), Stat Fax® 2600 Microplate washer (Awareness Technology Inc., Palm City, FL), bovine

serum albumin (BSA) (Fisher Scientific, Hanover Park, IL), DNA aptamer biotinylated modified 5'-/5Biosg/ GGG GTT GGG GTG TGG GGT TGG GG-3', DNA aptamer biotinylated amine modifier 5'- /5Bosg/GGG GTT GGG GTG TGG GGT TGG GG/3AmMO/ 3'(this sequence was used as the base for all the different aptamer-amphiphile used in this procedure, from Table 3 the amphiphiles used were C12B, NoSPRB and T10B), DNA aptamer 5'-/5Biosg/ TTT TTT TTT TTT TTT TTT TTT TT-3'all DNA purchased from Integrated DNA Technologies (Coralville, IA), sodium chloride crystal (NaCl) (Macron Fine Chemicals, Center Valley, PA), nuclease free water (Integrated DNA Technologies, Coralville, IA), orbital shaker (Fisher Scientific, Hanover Park, IL), Pierce® high sensitivity NeutrAvidin®- horseradish peroxidase (HRP) (Thermo Scientific, Rockford, IL), TMB stabilized substrate for HRP (Promega, Madison, WI) sulfuric acid (H_2SO_4) (Fisher Chemicals, Hanover Park, IL), and plate reader Bio-Tek Synergy HT (Winoski, VT).

3.2.2 Methods

The protein solution (β-lactoglobulin, α-lactalbumin, or ovalbumin) was dissolved in PBS (pH 7.4), 50 ng of protein was added to each reaction well and incubated overnight (16-18hrs) at 4°C. The plate was washed in the automatic plate washer with a PBS 0.05% Tween® 20 (3x 200 μL aspirating at the start, end and in between each 200 μL dispensing). The plate was incubated at room

temperature for 2 hrs with 200 μL of a 2% BSA solution in PBS in each well. The BSA solution was removed by inverting the plates. Aptamer solutions (0, 0.01, 0.1, 0.5, 1, 5, 10, 50, 100, 1000, 5000, 10000, 20000, 30000 nM) in 10 mM NaCl in water were added in to triplicate reaction wells (three wells per solution). The plate was then incubated at room temperature on an orbital shaker for 2 hours. The plate was then washed in the automatic plate washer (3x 200 μL). The NeutrAvidin HRP was added to the reactions wells, 50 μL of a 1 μg/mL solution in PBS, and the plate was incubated for 30 min at room temperature. After that, the plate was again washed in the automatic plate washer. The substrate TMB was then added, 100 μL per well, and the plate was allowed to oxidize for 20 min at room temperature. The stop solution, 1 M H_2SO_4 was added, and the plate them was read at 450 nm in the Bio-Tek Synergy HT plate reader. To measure the backgournd binding, the aptamer were added to the well without the protein solution and developed in an identical manner.

3.3 Aptamer-Amphiphile Synthesis

3.3.1 Materials

Amino modified DNA aptamer 5'GGG GTT GGG GTG TGG GGT TGG GG/3AmMO/ 3' (Integrated DNA Technologies, Coralville, IA), cetyl trimethylammonium bromide (CTAB) (Acros Organic, Morris Plains, NJ), *N,N*-

dimethylformimide (DMF) (Sigma-Aldrich, St Louis, MO), dimethyl sulfide (DMSO) (Sigma-Aldrich, St Louis, MO), trimethylamine (TEA) (Fisher Chemical, Hanover Park, IL), lithium perchlorate($LiClO_4$) (Sigma-Aldrich, St Louis, MO), acetone (Fisher Chemical, Hanover Park, IL), whatman syringe filters 0.45 μM pore size 25mm diameter (Sigma-Aldrich, St Louis, MO), methanol (Fisher Chemical, Hanover Park, IL), hexafluroisopropanol (HFIP) (Oakwood Products Inc., West Columbia, SC), zorbax C3 300SB column (4.6mmx 150mm x 3.5μm), copper grid 200 mesh (Ted Pella Inc., Redding, CA), acetonitrile (Sigma Aldrich, St Louis, MO), ammonium acetate (Sigma-Aldrich, St Louis, MO).

3.3.1 Methods

This method was followed in accordance with previous published method (Pearce and Kokkoli 2013) and with the assistance of Dr. Huihui Kuang. To start an aliquot of 100 nmol of aptamer was first mixed with 100 mM CTAB to forms ssDNA/CTAB complex. The suspension was then centrifuged and dried in the vacuum oven, room temperature, to remove the water. After 4 h drying time, the precipitate was dissolved ~150 μL of a mixture of DMF/DMSO (v/v 90/10). The hydrophobic tail, previously synthesized by the Kokkoli group (Craig et al. 2008), was also dissolved in DMF/DMSO, the amount of tail was calculated as being approximately 15 times the amount of ssDNA, and then 10 fold of the tail was added into the above ssDNA/CTAB solution. Finally, 8 μL of TEA was added and

the mixture was reacted overnight at 65 °C in a water bath. Then 5 times of the tail to the aptamer was added to the solution. After 4 h, the solvent was dried in an air stream until a final volume of about 100 μL. Then 900 μL of an ice cold solution of $LiClO_4$ in acetone and 100 μL of water was added to the mixture. The mixture was then put in the freezer at -20 °C for 15 min and then centrifuged for 10 min to isolate the precipitation (ssDNA amphiphile and unreacted ssDNA). Water was added to wash the precipitate in three separate additions, 400 μL, 200 μL and 200 μL repeating the centrifugation and supernatant removal process in between each addition. The sample was then purified by removing the unreacted aptamer, using reverse phase HPLC. HPLC conditions: Zorbax C18 300 A SB column, 5-90 % B over A for 25 min, buffer A: water, 10 % methanol, 100mM HFIP and 14.4 mM TEA, buffer B: methanol, 100mM HFiP, 14.4mM TEA. The molecular weight of the aptamer-amphiphile was verified by Dr. Huihui Kuang using liquid chromatography-mass spectroscopy (LC-MS).

The morphologies of ssDNA-amphiphiles were analyzed using cryogenic transmission electron microscopy (cryo-TEM). An aliquot of 4.5 μL amphiphile solution was deposited onto a treated glow discharge cooper grid, the treatment was performed in a Vitrobot for 60 seconds (4 sec blot time, 0 offser, 3 sec wait time, 3 sec relax time, ambient humidity). The grids were kept under liquid nitrogen until they were ready to be read by the Tecnai G2 Spirit TWIN 20-

1230kV/LaB6 TEM operated with an acceleration voltage of 120keV. An Eagle 2k CCD camera was used to capture the images.

3.4 Liquid Crystal Sensors

3.4.1 Materials

Microscope glass slides, glass petri dishes, glass coplin staining jar, sulfuric acid (Fisher Chemical, Hanover Park, IL), hydrogen peroxide 35 wt% solution in water (Acros Organics, Morris Plains, NJ), ethanol 200 proof (Decon Labs, King of Prussia, PA), methanol (Fisher Chemical, Hanover Park, IL), octadecyltrichlorsilane 95% (OTS) (Acros Organis, Morris Plains, NJ), heptane 99% (Alfa Aesar, Ward Hill, MA), dichloromethane (Acros Organics, Morris Plains, NJ),squared CU grid 100 mesh (Fisher Scientific, Hanover Park), 4'-pentyl-4-biphenylcarbonitrile 98% (5CB) (Sigma Aldrich, St Louis, MO), sodium dodecyl sulfate (Fisher Scientific, Hanover Park, IL).

3.4.2 Methods

The glass slides were cleaned in a piranha solution, 70% sulfuric acid and 30% hydrogen peroxide, for 1 h at 80 °C. The slides were then rinsed subsequently with water, ethanol, and methanol. The slides were then dried with nitrogen gas and heated at 110 °C for 2 hrs in a gravity oven. The slides were stored in a vacuum desiccator until next use. The hydrophobic coat was

deposited by soaking the slides in a 0.5 mM OTS solution in heptane for 30 minutes. Slides were them rinsed with dichloromethane, dried with nitrogen and stored under vacuum. The grids were cleaned with dichloromethane, ethanol and methanol and heated at 110 °C for 24 hrs. To assemble the liquid crystal sensor, the previously prepared TEM grid was placed on the OTS-treated glass slide, Figure 10, and 1 μL of the 5CB was place in the grid. The cell was heated for 30 min at 50 °C, and then it was subjected to the target analyte solution for 20 min. The cell was then observed in the polarizing microscope, plane-polarized light in transmission mode on a Nikon Optiphot light microscope with crossed polarizers. The source light in the microscope was set at 50% of full illumination and the aperture used was set at 10%. The images were captured using a Canon SL1 digital camera. To evaluate the self-assembly of the liquid crystal the cell was exposed to water, 2.2 mM SDS solution and air. The aptamer-amphiphile was then added to the cell and let equilibrate for 20 min, after that the image was observerd and the β-lactoglobulin solution were added to the cell and let it equilibrate for 20 more minute before observing the image. The same procedure was done for a different protein, ovalbumin. Another test to evaluate the LC sensor was to use a mix of the target protein β-lactoglobulin and a random protein, ovalbumin to verify the specificity of the sensor. To evaluate the limit of detection a fixed amount of aptamer-amphiphile was tested at several concentrations of β-lactoglobulin solutions.

Some preliminary surface swab-testing was also performed, 5 mL of a 10 μM β-lactoglobulin solution (in 10 mM NaCl) was spotted on three different surfaces, stainless steel, high density polyethylene (HDPE) and ceramic tile. The solutions were let to dry for about 30 min and the excess was patted dry with a paper towel. The surface was swabbed using a cotton swab for approximately 15 seconds and the swab was dipped in to 10 mL of 10 mM NaCl and mixed by hand. The resulting solution was added to the LC cell containing the aptamer-amphiphile, and the image was obtained using the polarizing microscope. The results for this test is disposed on Appendix C.

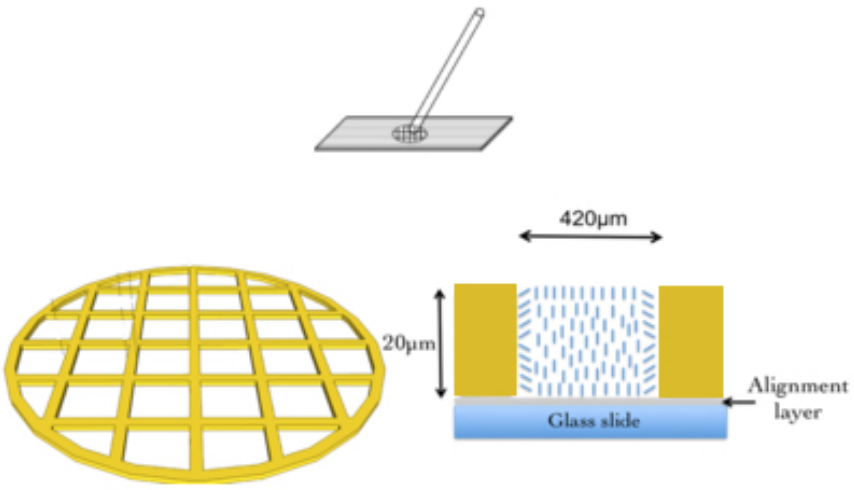

Figure 10 Representation of the assembly of the liquid crystal sensor. Adapted from: (Brake and Abbott 2002b; Iglesias et al. 2012)

4. Results and Discussion

4.1 Circular Dichroism

Circular dichroism spectroscopy was used to evaluate the tridimensional structure of the ssDNA aptamer. Aptamers can associate in self-assembly tridimensional structures called a G-quadruplex by the interaction of four guanines through hydrogen bonds (Bryan and Baumann 2010). There are two kinds of G-quadruplex, called parallel and anti-parallel, that can be differentiated by CD spectroscopy based on its maximums and minimums peak wavelengths, Table 4.

Table 4 Theoretical peaks wavelengths for parallel and anti-parallel G-quadruplexs structures(Kypr et al. 2009) .

	Maximums		**Minimum**
Parallel	210 nm	260 nm	240 nm
Anti-parallel	210 nm	290 nm	260 nm

This structure is more prominent in pure water or in aqueous solutions. The cations present in the solution can affect the stabilization of this structure. Based on that several electrolytes were tested to determine which one would give the more stable G-quadruplex structure for the aptamer, Figure 11.

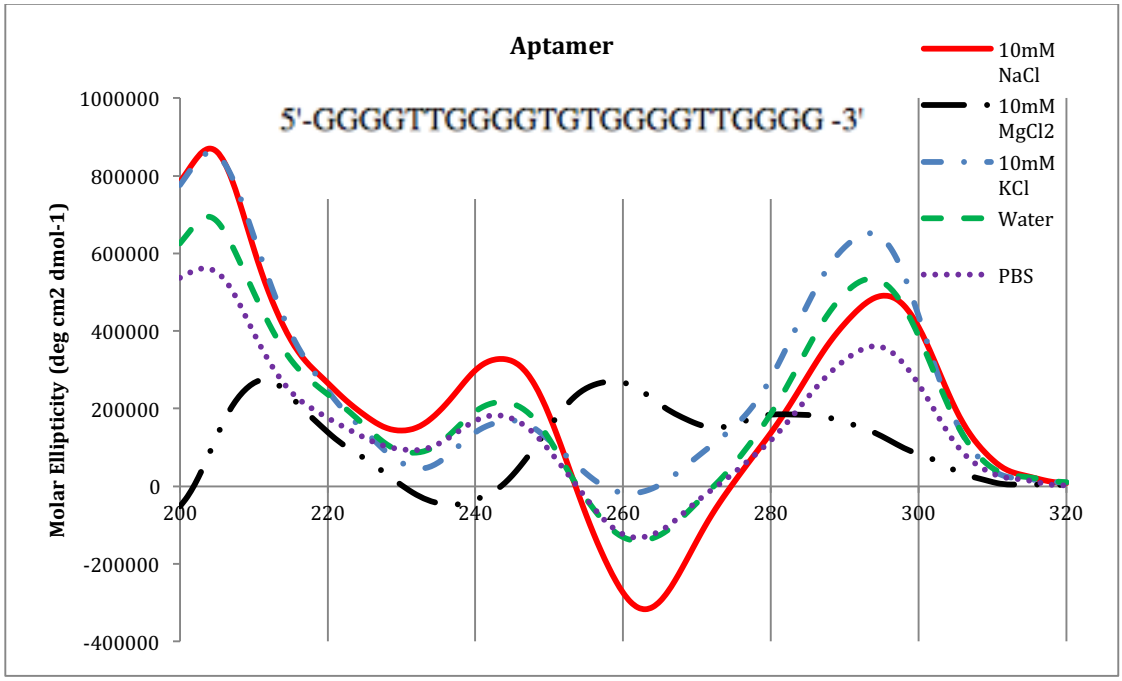

Figure 11 Circular dichroism spectrum for the aptamer in several electrolytes.

As seen in Figure 11, the electrolyte that gives the spectrum of a characteristic G-quadruplex (maximums at 210 and ~290 nM and minimum at approximately 260 nm), in this case an anti-parallel, is at 10 mM NaCl. Thus based on that, all the applications for the aptamer would be performed using this electrolyte.

Considering that the method of choice for the binding evaluation was a modified ELISA procedure, the aptamer had a biotin molecule attached to the 5' end. The tridimensional structure of this was also evaluated by CD, and the result can be seen in Figure 12.

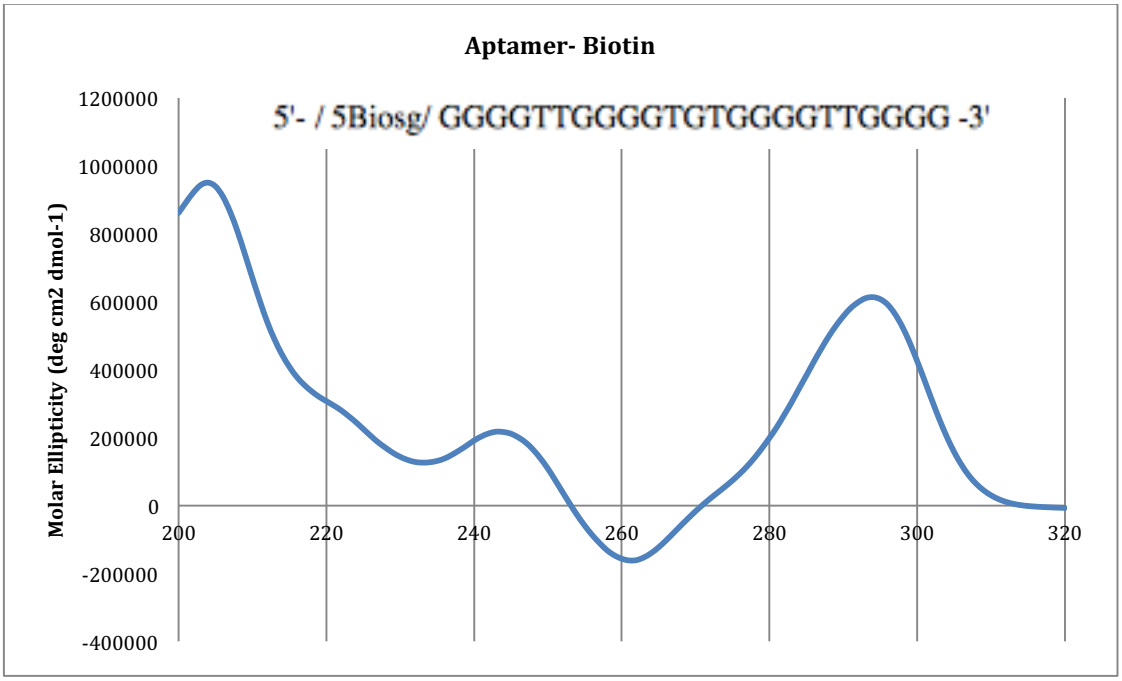

Figure 12 CD spectrum for the aptamer with a biotin molecule on the 5' end.

The presence of a biotin molecule on the 5’ end did not change the overall structure of the G-quadruplex. The biotinylated aptamer still holds an antiparallel G-quadruplex, using 10 mM NaCl as the electrolyte.

Initially, the ssDNA-amphiphile that was synthesized was the one with a C12, Table 3. For that synthesis the aptamer was ordered from IDT with an amine molecule on the 3’ end. The secondary structure was evaluated by CD after dissolving the amphiphile in 10 mM NaCl, this is showing in Figure 13.

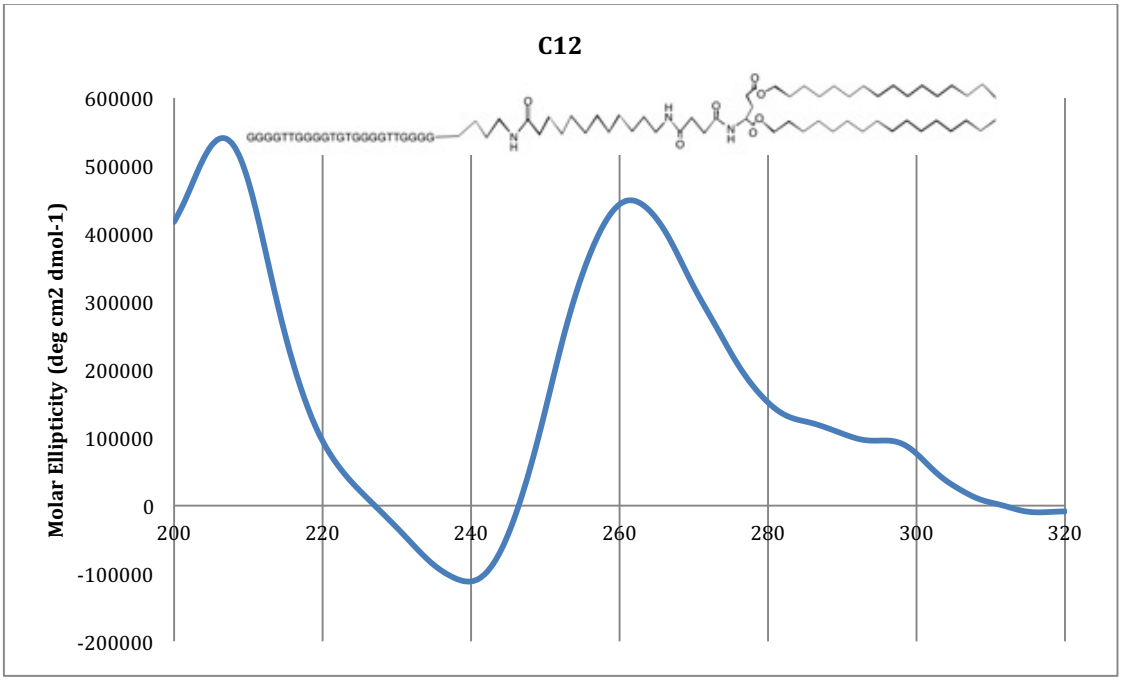

Figure 13 CD spectrum of the ssDNA amphiphile with the C12 spacer.

Observing the maximums and minimums in Figure 13, it is possible to conclude that the C12 spacer amphiphile presents a parallel G-quadruplex, with maximums at 210 and 260 nm and a 240 nm minimum. From that result, the synthesis was performed in the same way for all of the other aptamer-amphiphiles.

Three ssDNA-amphiphiles were synthesized and the CD spectrum measured, all using 10 mM NaCl as the solvent. Since those amphiphiles would also be used in ELISA tests they also had a biotin molecule attached to the 5' end. For the amphiphile synthesis it is also necessary to have an amine molecule

where the tail would be attached. In this case those were ordered from IDT with an amine molecule at the 3' end. The ssDNA-amphiphiles that were synthesized were, C12 spacer amphiphie (C12), no spacer amphiphile (NoSPR), and T10 spacer amphiphile (T10) (Table 3).

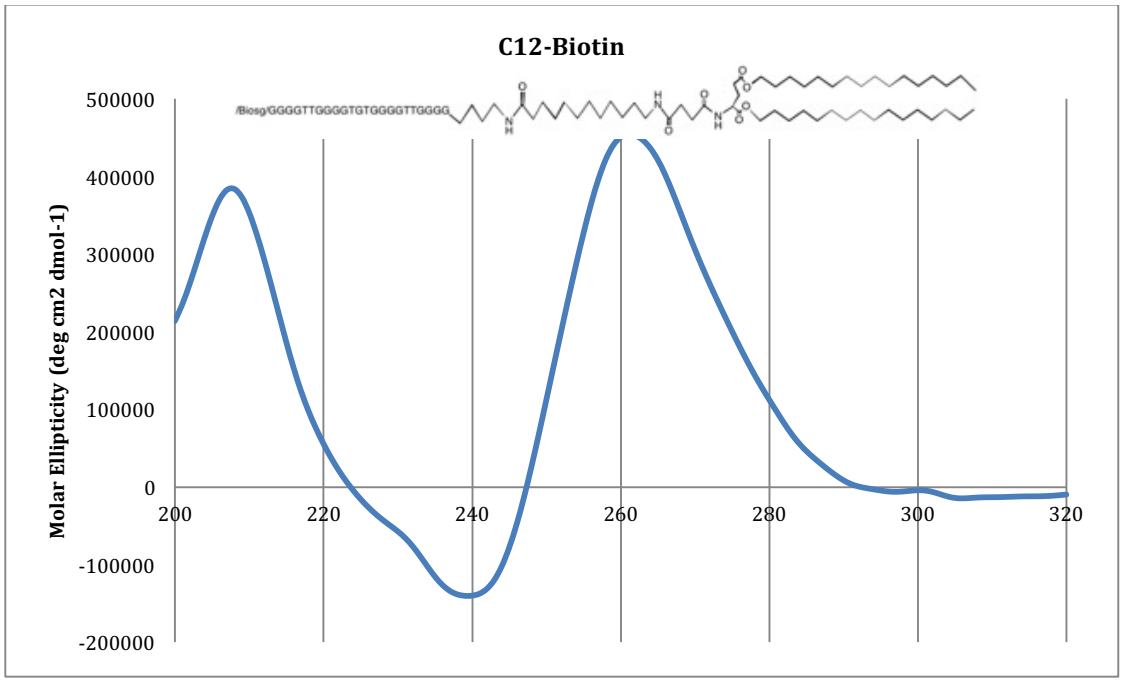

Figure 14 Circular dichroism spectrum for the biotinylated C12 ssDNA-amphiphile

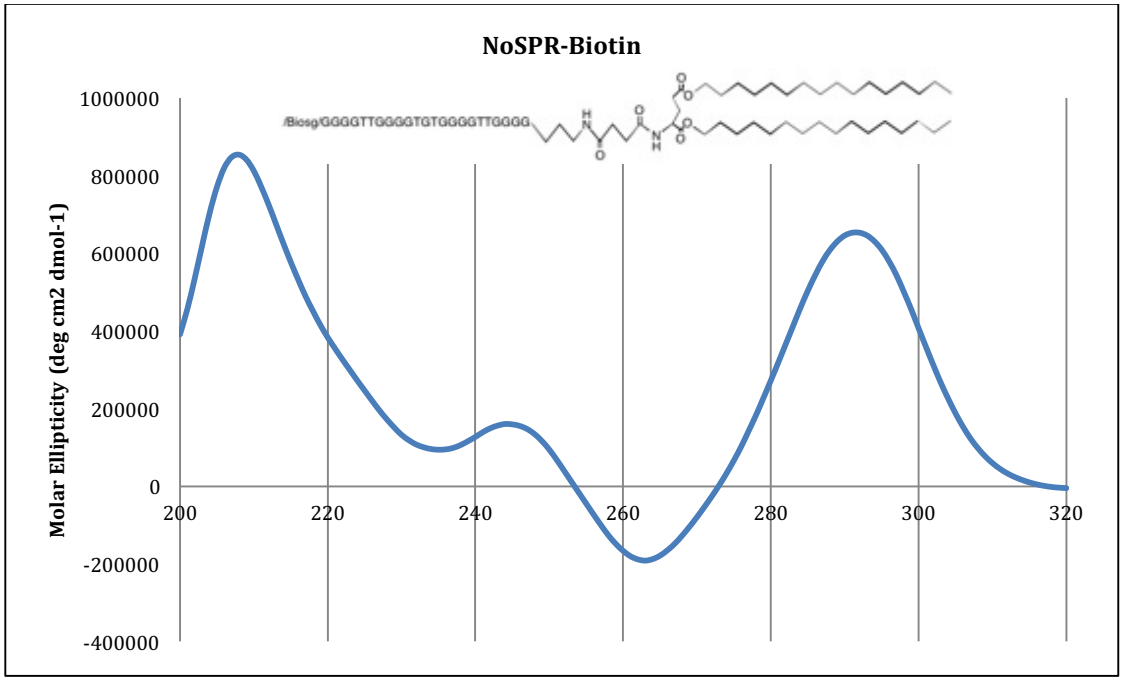

Figure 15 Circular dichroism spectrum for the biotinylated NoSPR ssDNA-amphiphile

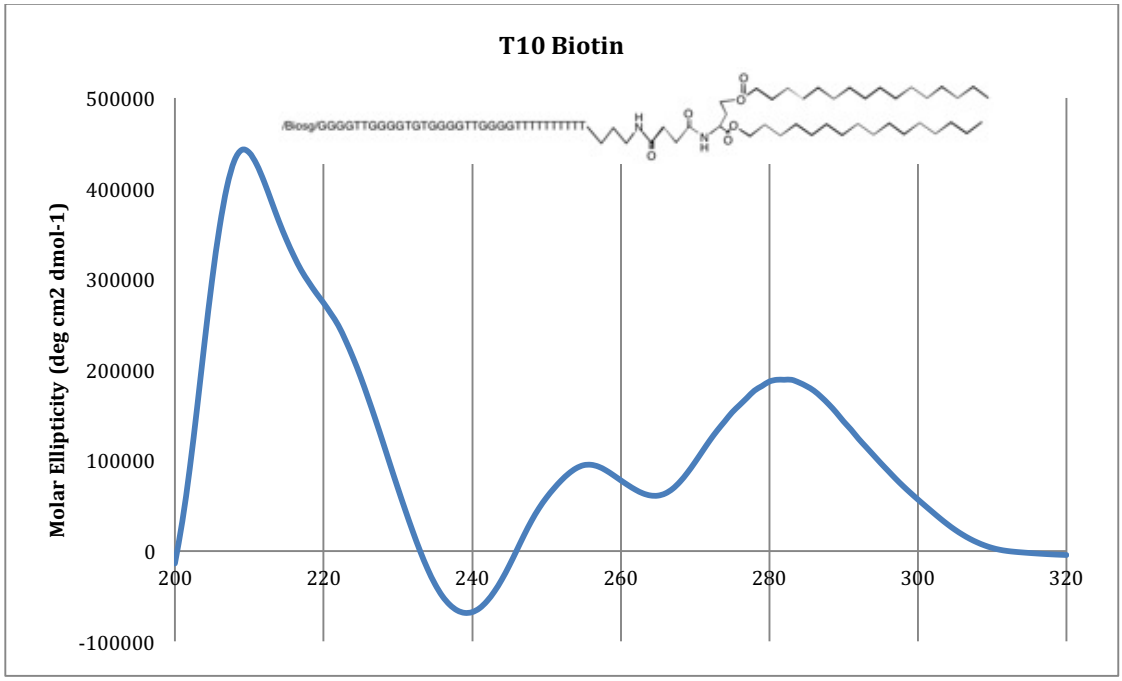

Figure 16 Circular Dichroism spectrum for the biotinylated T10 ssDNA-amphiphile

As it was expected from the non-biotinylated C12 amphiphile, Figure 13, the C12-biotin has the same parallel G-quadruplex structure as shown in Figure 14. On the other hand, the NoSPR kept the free aptamer conformation, Figure 15, antiparallel G-quadruplex. The T10 biotin presents what can be called a hybrid structure, having same traces of parallel G-quadruplex, minimum at 240 nm and maximum at 210 and 260 nm. But it also has a maximum around 290 nm that is a characteristic of antiparallel G-quadruplex as seen in Figure 16.

For the liquid crystal application, the presence of the biotin molecule is not necessary so the ssDNA-amphiphile that presented the best binding constant,

results showed in section 4.3, in this case the NoSPR aptamer-amphiphile was synthesized without the biotin molecule and the structure was also evaluated using CD.

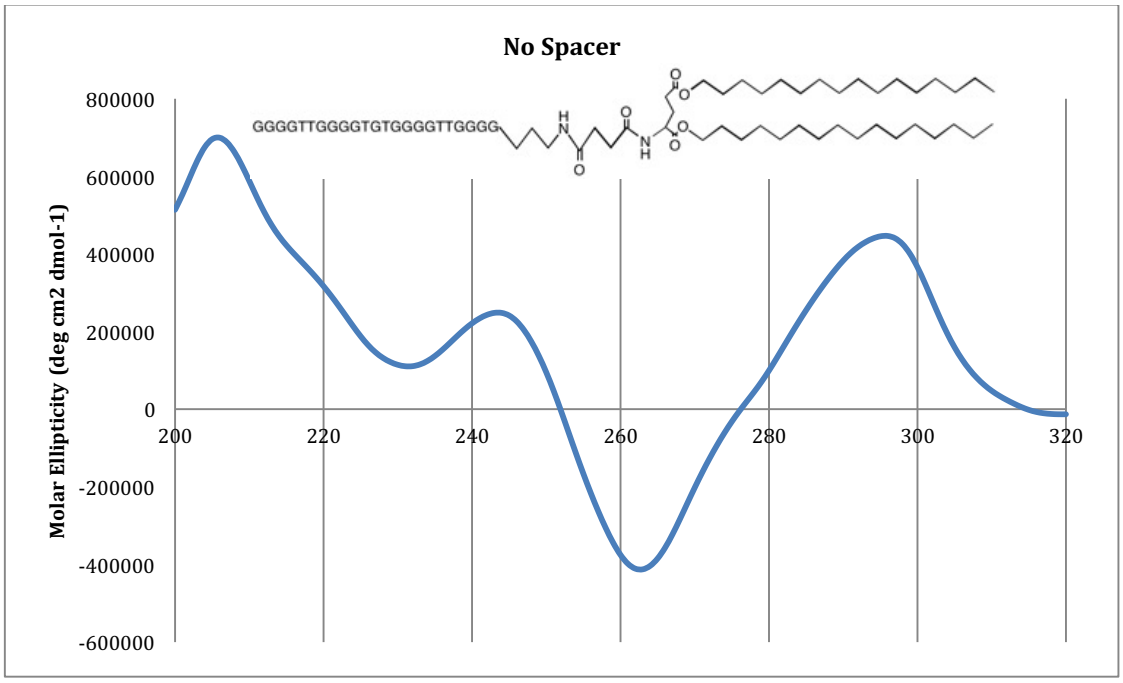

Figure 17 Circular dichroism spectrum for the NoSPR ssDNA-amphiphile

As seen in Figure 17 the NoSPR ss-DNA-amphiphile held the antiparallel G-quadruplex structure when the synthesis was performed without the biotin molecule, presenting the characteristic maximums and minimums in the spectrum, respectovey at 210 and 290nm maximus and minimum at 260 nm.

4.2 Evaluation of Binding Constant

The ELISA type procedure but using aptamer instead of antibody (ELASA) was the method of choice to evaluate the binding between the aptamer and protein, based on previously published work (Shroff et al. 2012). All the samples, the aptamers and aptamer-amphiphiles, were tested in triplicate using the same concentrations range namely, 0, 0.01, 0.1, 0.5, 1, 5, 10, 50, 100, 1000, 5000, 10000, 20000, 30000 nM. The binding evaluation study has as a result the dissociation constant (K_d), the smaller the constant the greater affinity of the aptamer to the target protein.

From the ELASA experiment the data collected is absorbance, collected using a UV-Vis spectrophotometer at 450 nm. In all of the following sections, a plot is shown of absorbance (B) *vs* log concentration (A) of aptamer or aptamer amphiphile with the protein. This data was then used in MatLab to solve for the two constant in Equation 3 below, the binding constant K_d and the max intensity Bmax. From this and assuming concentrations over the whole interval fits a sigmoid shape line (Klotz plot) is created by MatLab.

Each graph legend lists the binding constant K_d and the Bmax. It should be noted that the plot is absorbance *vs* log concentrations which is useful in studying protein binding (Obenauer and Yaffe 2004).

The predicted absorbance *vs* log concentration are in Appendix B along with the actual triplicate results.

$$B = \frac{B_{max}\, x\, [A]}{(K_d + [A])} \quad (3)$$

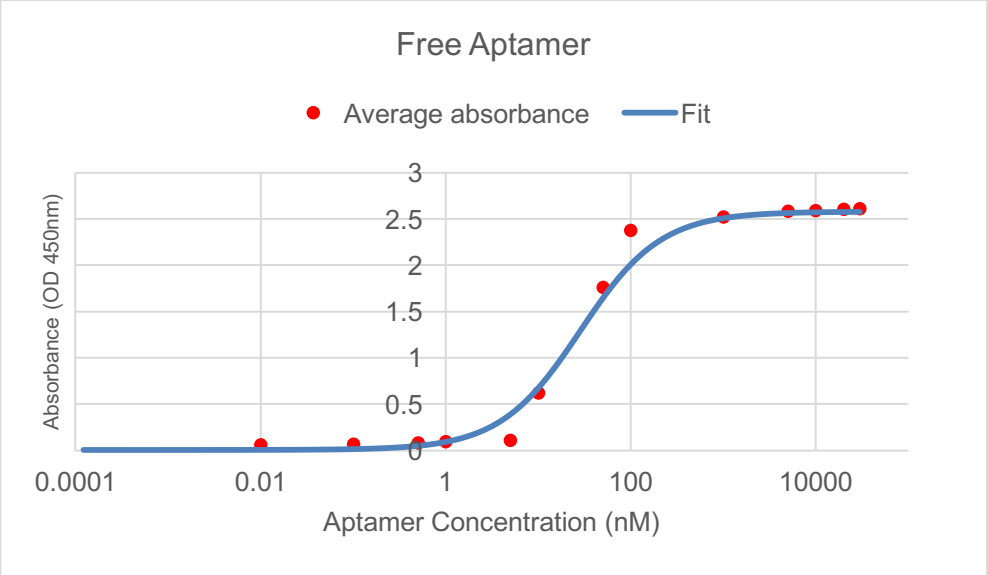

Figure 18 Non-linear fit, based on equation (3), obtained for the aptamer and β-lactoglobulin, and experimental average absorbance. Kd=2.88 ± 0.056 nM, Bmax=2.58 ± 0.02.

From this, the K_d for aptamer was calculated as K_d=2.88±0.056 nM. This value gives evidence that the aptamer has a high affinity towards the target. To further verify this sequence potential application, two control tests were performed, one using a randomized (not G-quadruplex former) sequence (5'-/5Biosg/ TTT TTT TTT TTT TTT TTT TTT TT-3') and β-lactoglobulin (Figure 18) and a second test using two others proteins, in this case α-lactalbumin (Figure 19) and ovalbumin (Figure 20). The ELASA test was performed in the same

matter as for the target protein, β-lactoglobulin, and the original aptamer sequence.

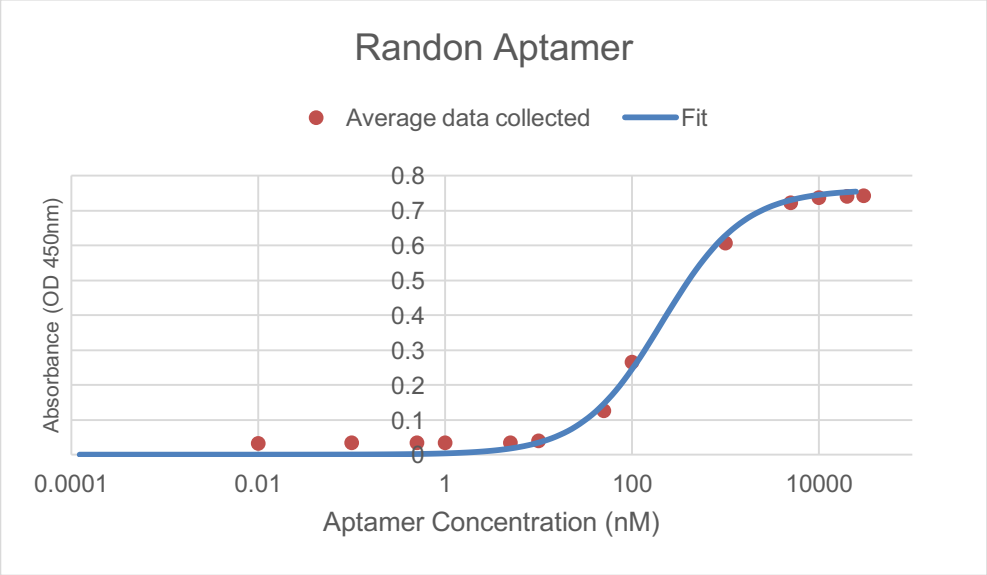

Figure 19 Non-linear fit, based on equation (3), obtained for the random aptamer and β-lactoglobulin, and experimental average absorbance. Kd= 246 ± 7.23 nM, Bmax=0.719±0.01

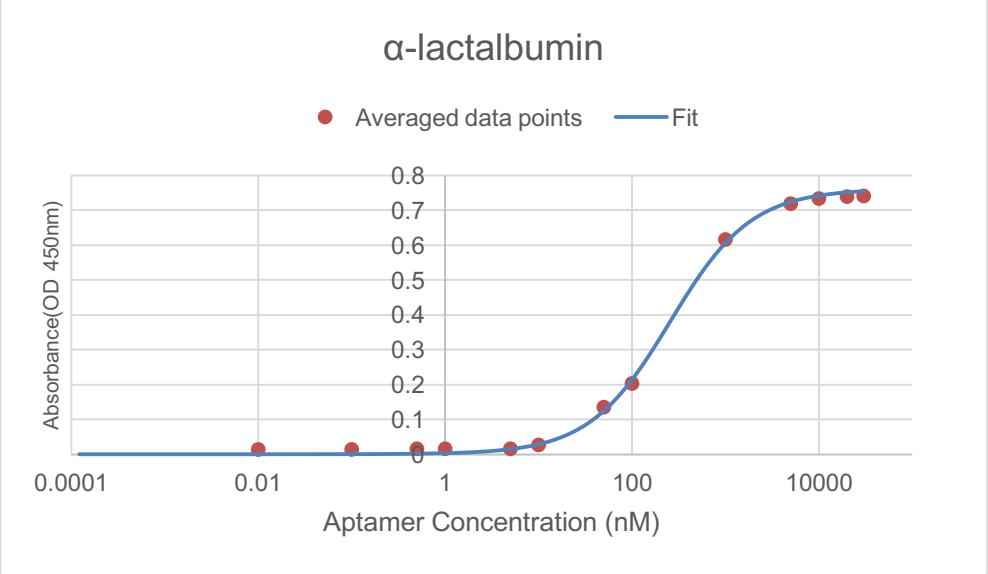

Figure 20 Non-linear fit, based on equation (3), obtained for the aptamer and α-lactalbumin, and experimental average absorbance. Kd= 259 ± 13.2 nM, Bmax=0.743 ± 0.0156

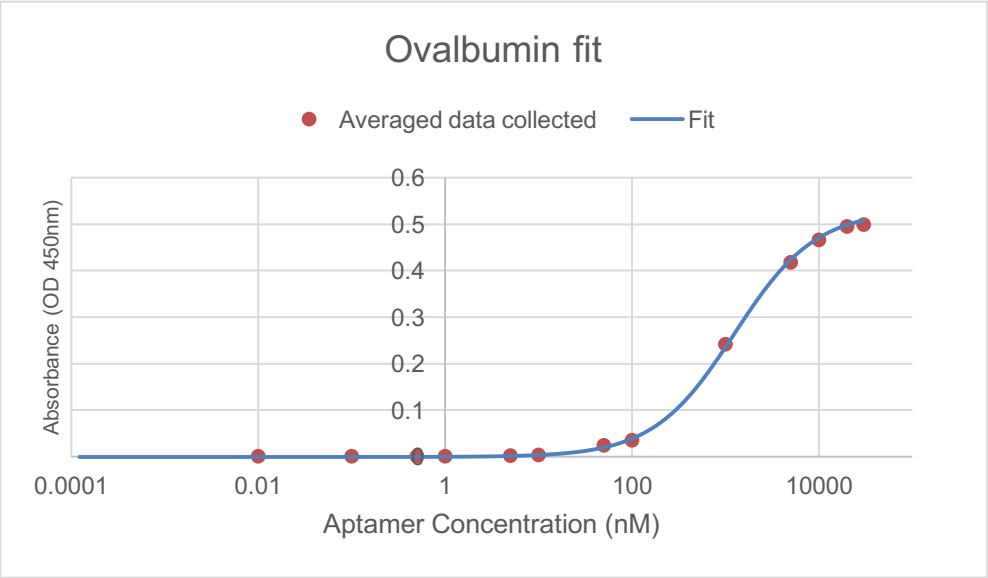

Figure 21 Non-linear fit, based on equation (3), obtained for the aptamer and ovalbumin, and experimental average absorbance. Kd=1190 ± 90 nM, Bmax=0.519 ± 0.0174.

As seen in Figures 19, 20 and 21 there is some binding occurring between the random aptamer sequence and the target protein and also between other proteins to the selected aptamer sequence. But observing the K_d values, 246 nM for the random aptamer sequence, 259 nM for α-lactalbumin and 1190 nM for ovalbumin, it can be seen that those values are much larger than the K_d obtained for the selected aptamer sequence and the target protein, β-lactoglobulin, K_d=2.88 nM. This indicates that this pair has a much larger affinity, making this the best choice to use with the sensor development.

From that result, it was possible to conclude that the sequence of choice (5'-GGG GTT GGG GTG TGG GGT TGG GG-3') is a desirable one to be used to

synthesized the aptamer-amphiphiles and afterward applying it on the liquid crystal sensor.

Three amphiphiles were synthesized and evaluated in relation to binding affinity to β-lactoglobulin. The aptamer-amphiphiles synthesized were C12B, T10B, and NoSPRB (Table 3). In the Figures below, 22,23 and 24 it is possible to see the fits and K_d obtained from this experiment (the numbers for the K_d calculation and for the fit are in appendices B).

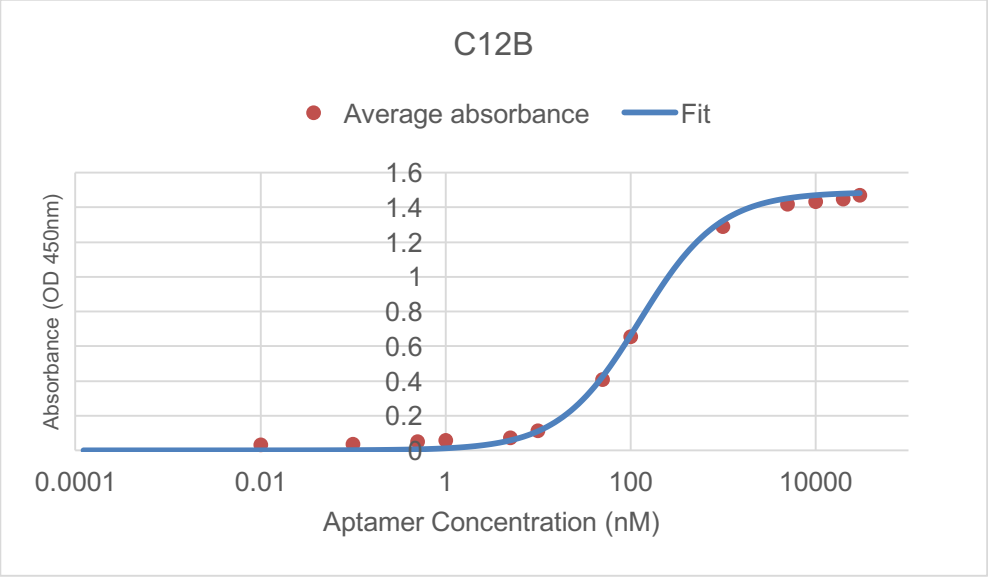

Figure 22 Non-linear fit, based on equation (3), obtained for the aptamer-amphiphile C12B spacer and β-lactoglobulin, and experimental average absorbance. K_d=134 ± 7.94 nM, Bmax=1.43 ± 0.006

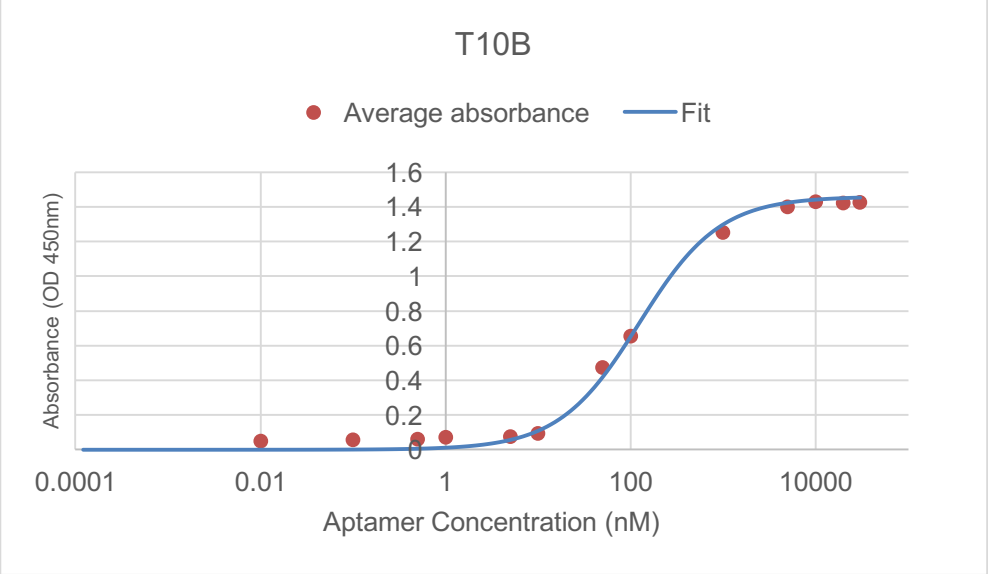

Figure 23 Non-linear fit, based on equation (3), obtained for the aptamer-amphiphile T10B spacer and β-lactoglobulin, and experimental average absorbance. K_d= 127± 4.58 nM, Bmax=1.38 ± 0.015

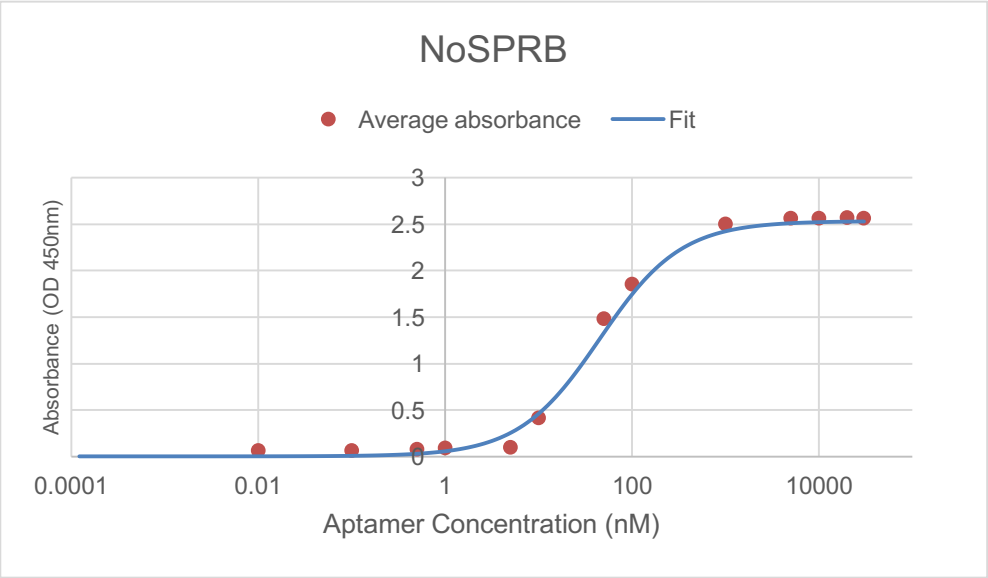

Figure 24 Non-linear fit, based on equation (3), obtained for the aptamer-amphiphile NoSPRB and β-lactoglobulin, and experimental average absorbance. K_d= 45 ± 1.68nM, Bmax= 2.53 ± 0.02

The amphiphiles dissociation constant C12B, T10B and NoSPRB, respectively are 134 nM, 127 nM and 45 nM. Thus using the same rationale previously illustrated, the lower the constant better the binding, the amphiphile without a spacer between the ssDNA head the carbonic tale is the one with more affinity to the target protein and consequently will be the one used for study with the liquid crystal sensor.

Observing the results obtained it is possible to hypothesize that the target protein has a good binding preference for the DNA aptamer that forms a specific G-quadruplex structure, in this case, an antiparallel structure. This can be concluded because it has a high affinity for the aptamer, K_d=2.88 nM, that forms

an antiparallel G-quadruplex and also between the three amphiphiles synthesized the one with the highest affinity, NoSPRB K_d=45 mM, is the non-spacer ssDNA-amphiphile that would be the only one among the synthesized ones that have an antiparallel structure.

4.3 Aptamer-Amphiphile synthesis

4.3.1 Cryogenic transmission electron microscopy Cryo-TEM

The synthesized ssDNA-amphiphiles were evaluated using Cryo-TEM microscopy, this analysis verified the tri-dimensional shape and size of the amphiphile. There are several works that have been done exploring the potential of ssDNA amphiphiles to self-assemble in three dimensional structures that do not follow the Watson-Crick base paring. The Kokkoli group (2015) had previously observed that variations on the length of the ssDNA head group and the tail characteristics may affect the observed structure. The three major structures observed by this work were, micelles, tapes and nanotubes.

Some of the findings of these works are that ssDNA containing guanine bases that were conjugated to the tail using a carbonic spacer, in the scope of this work a C12 spacer, may form micelles, tapes and also nanotubes. The amphiphile synthesized in this work, C12 Spacer Amphiphile, formed both micelles and nanotubes, Figure 25. A ssDNA amphiphile with no spacer between the tale and the DNA head group, NoSPR, was also synthesized and evaluated

in this work. This amphiphile formed micelles, as shown in Figure 26, as expected based on previously published work (Pearce and Kokkoli 2015). In this work an amphiphile synthesized using T10 as the spacer was also synthesized and as expected it formed micelles as showed in figure 27 (Waybrant et al. 2014).

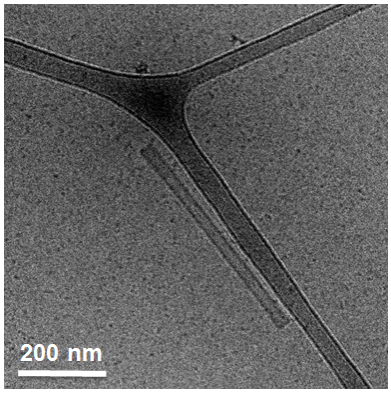

Figure 25 Cryo TEM image of the nanotube formed by the ssDNA amphiphile with C12 spacer. Tube dimensions: diameter: 30.8 ± 1.8nm and length: 80-520nm. Image was collected by Dr. Huihui Kuang.

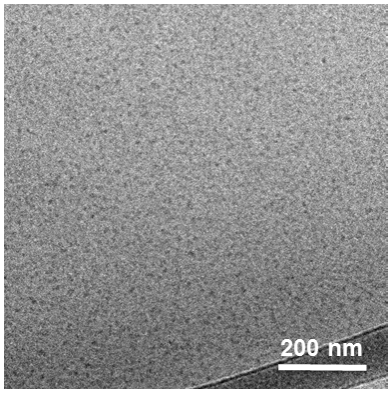

Figure 26 Cryo TEM image of the micelles formed by the ssDNA amphiphile with no spacer, NoSPR. Micelle dimensions: diameter: 12.2±0.8nm. Image was collected by Dr. Huihui Kuang.

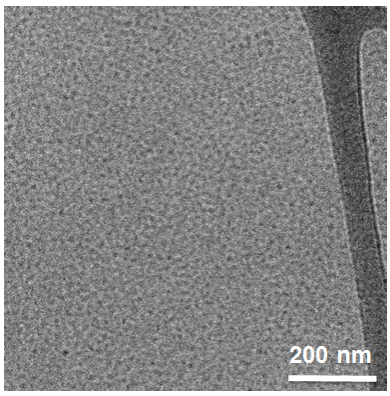

Figure 27 Cryo TEM image of the micelles formed by the ssDNA amphiphile with 10T spacer, T10. Micelle dimensions: diameter: 12±0.9nm. Image was collected by Dr. Huihui Kuang.

4.4 Liquid Crystal (LC) Sensor

The liquid crystal sensors were developed based on previously published work (Brake and Abbott 2002b). A glass slide cleaned with piranha solution and treated with a OTS homeotropic alignment layer was used as the bases for the sensor. A previously prepared TEM grid was set on top of the treated glass slide and the liquid crystals 5CB were confined in the grid. Initially the sensor was subjected to different solutions, water, 2.2 mM SDS and air, to verify if the sensor would behave as expected.

According with the literature, when a liquid crystal is supported in a glass treated with an OTS homeotropic alignment layer is exposed to air, and to certain concentrations of surfactant, it will self-assembly in a homeotropic arrangement. A dark image will be overserved using a polarizing microscope. When the same

sensor is exposed to water the LC will arrange in a parallel alignment which will give a bright image in the the polarizing microscope (Brake and Abbott 2002a).

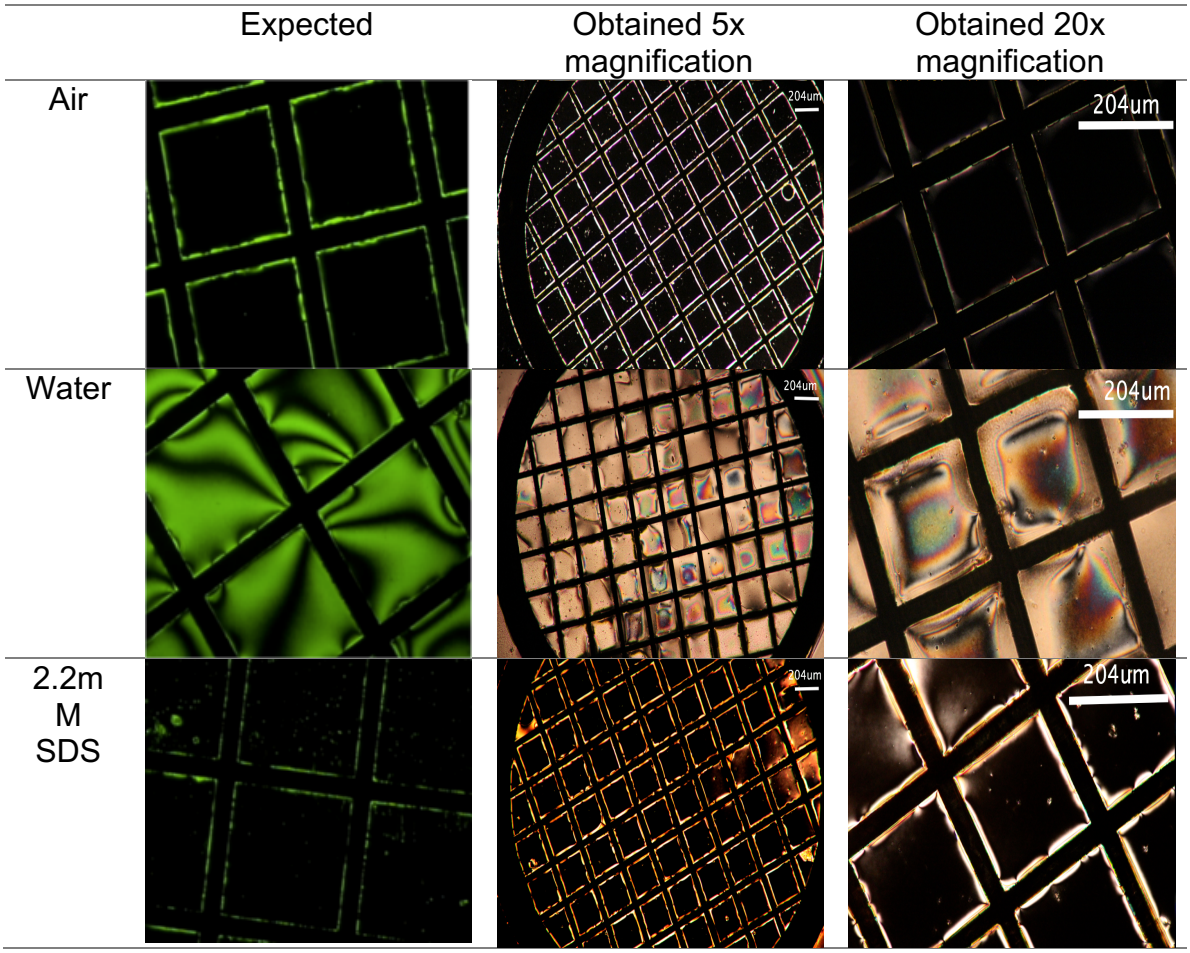

Figure 28 Optical images of the 5CB LC confined to a copper grid supported on a OTS treated glass under the polarizing microscope. The images reflect the LC exposed to air, water and 2.2 mM SDS. The expected column was adapted from (Iglesias et al. 2012), The images on the obtained columns were obtained using a Nikon microscope with transmitted polarized lights and a digital Canon camera.

The Figure 28 above demonstrates the technique utilized to clean and prepare the slides were successful, as all the obtained images matches what were expected for that designated arrangement. The work was followed by subjecting the LC sensor to the aptamer-amphiphile, the NoSPR amphiphile since it was the one with the highest affinity to β-lactoglobulin. In this case the aptamer-amphiphile would have similar characteristics to the surfactant, a polar head and a non-polar tale, the expected images would be black. For this arrangement to be used as a sensor, it was necessary to verify that once the aptamer-amphiphile, NoSPR, is in the presence of the target, β-lactoglobulin, the image would change to bright. These two hypothesis were tested and the results can be seen in the Figure 29 below.

	Expected	Obtained 5x magnification
NoSPR Aptamer-Amphiphile	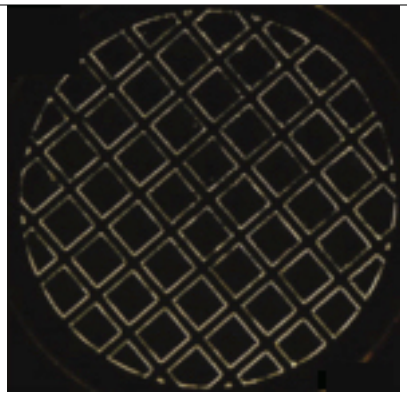	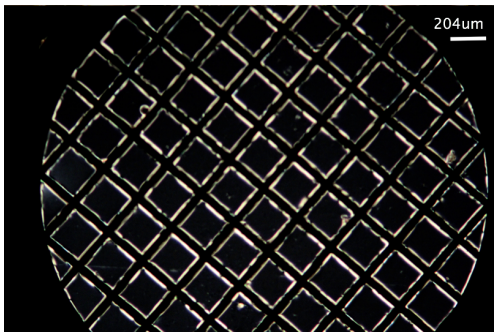
NoSPR Aptamer-Amphiphile + β-lactoglobulin	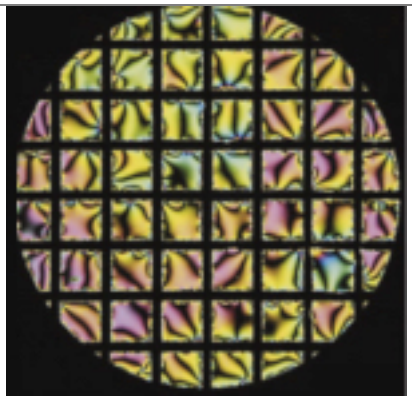	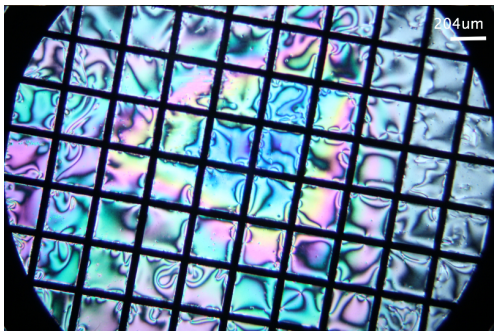

Figure 29 Optical images of the 5CB LC confined to a copper grid supported on a OTS treated glass under the polarizing microscope. The images reflect the LC exposed to the NoSPR aptamer-amphiphile and subsequently to the β-lactoglobulin, the target protein. The expected column was adapted from(Lockwood et al. 2008). The images on the obtained column were obtained using a Nikon microscope with transmitted polarized light and a digital Canon camera.

The optical images in Figure 29 confirms the hypothesis that once the LC is exposed to the aptamer-amphiphile, NoSPR, the image observed would be dark, and the subsequently exposure to the target protein, β-lactoglobulin, would make the image to change to bright.

To further evaluate the hypothesis of this LC assembly to be used as sensor, the limit of detection was evaluated. A fixed amount of aptamer-

amphiphile, was added to several LC sensors and let it sit for 20 min at room temperature, all of these were observed under to polarizing microscope to verify that the image was dark. Following this preliminary evaluation the cells were subjected to several concentrations of β-lactoglobulin solutions. The cells stayed in the protein solution for 20 min and then it was observed under the polarizing microscope.

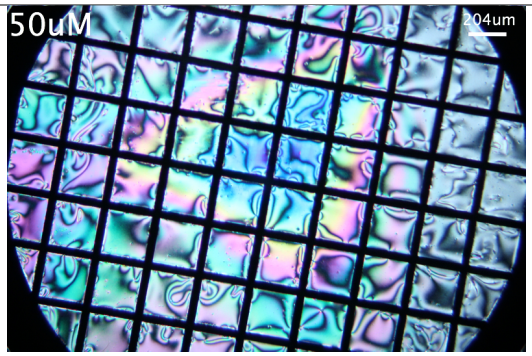
50uM
204um

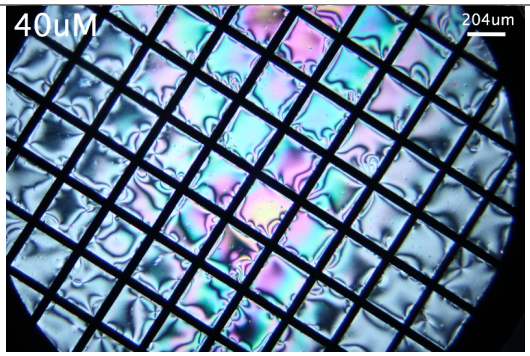
40uM
204um

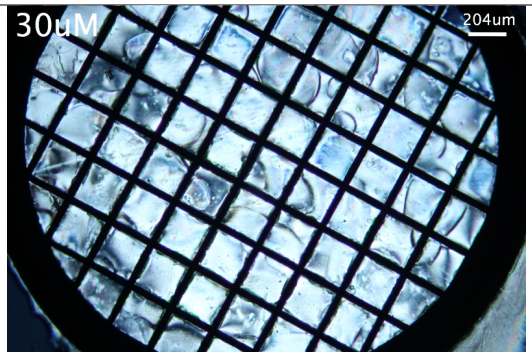
30uM
204um

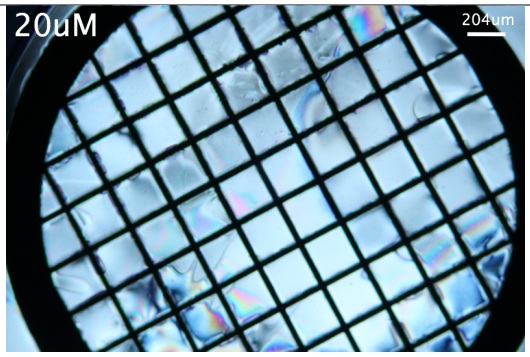
20uM
204um


10uM
204um

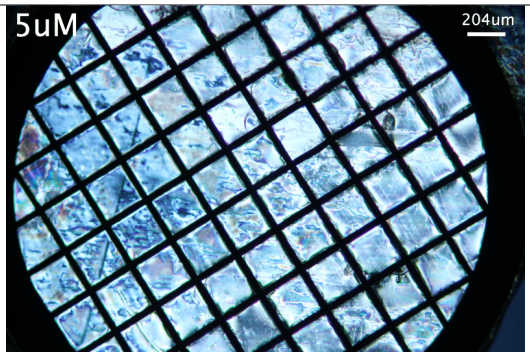
5uM
204um

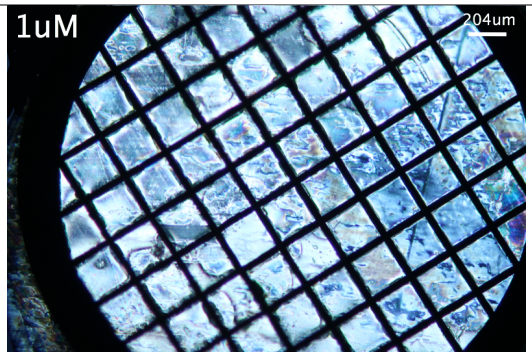
1uM
204um

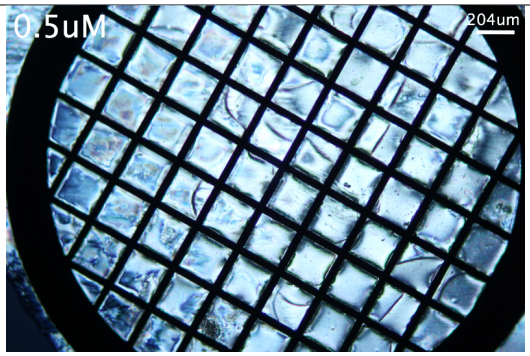
0.5uM
204um

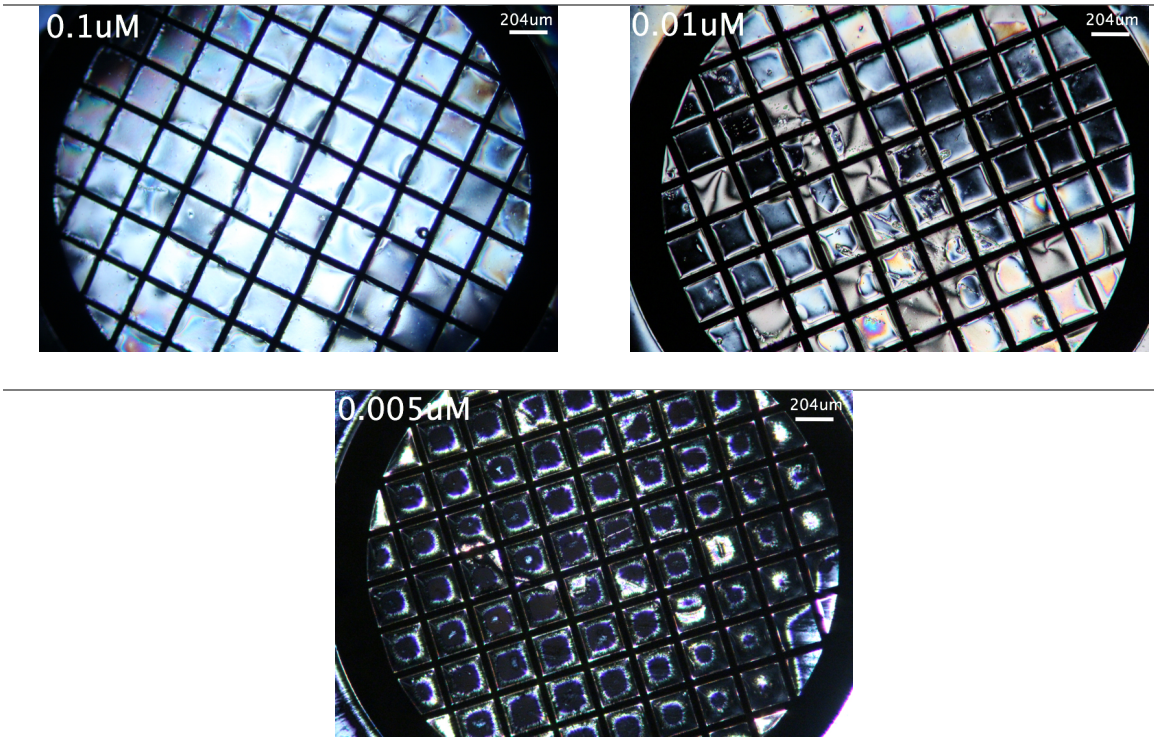

Figure 30 Optical images of the 5CB LC confined to a copper grid supported on a OTS treated glass under the polarizing microscope. The images reflect the LC exposed to the NoSPR aptamer-amphiphile and subsequently to several β-lactoglobulin solutions in 10mM NaCl, ranging from 50μM to 0.005μM. The images were obtained using a Nikon microscope with transmitted polarized light and a digital Canon camera.

The images Figure 30 show that the LC assembled sensor has capabilities to qualitatively detect a target protein at different concentrations. To evaluate the limit of detection the criteria used was that once the image presents the majority of the squares dark the concentration would be considered the limit of detection. In this case the limit of detection was established as being 0.01 μM, 18.4 ng of β-lactoglobulin, or 1.84 ppm.

Comparing this limit of detection with some commercial available ELISA tests for β-lactoglobulin overall the obtained result is higher. For example, for the kit sold be Crystal Chem- High Perfomance assays, the limit of detection is 0.312 ppm. The kit sold by Biomatik has a much lower limit of detection 0.000073 ppm (Biocompare.com; Crystal Chem). Even though the obtained limit of detection is higher, the method developed by us is faster, simpler and can be easily automated to be used in food processing facilities. On top of that, the majority of the ELISA tests commercially available are developed to be used for food products not on surfaces whereas the intent of the one developed in this work is to be used on surfaces.

The LC sensor containing the aptamer-amphiphile was subjected to a different protein, ovalbumin, this procedure was conducted in the same manner as the procedure for β-lactoglobulin. Observing the results in Figure 31 it is possible to see that the binding affinity that the aptamer has to the protein affects the results in the liquid crystal sensor. The aptamer has a K_d of approximately 2.88 nM to the β-lactoglobulin and a K_d of approximately 1190 nM to the ovalbumin. This indicates that the binding affinity to the ovalbumin is too low so that explains why the image obtained is dark as if the aptamer-amphiphile was not being in contact with a target instead of the bright image observed for the target that has good binding affinity, β-lactoglobulin.

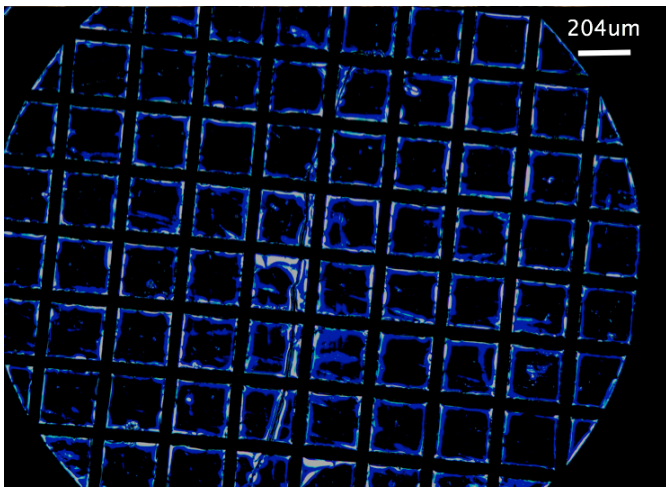

Figure 31 Optical images of the 5CB LC confined to a copper grid supported on a OTS treated glass under the polarizing microscope. The images reflect the LC exposed to the aptamer-amphiphile and subsequently to 10μM ovalbumin solution. The image was obtained using a Nikon microscope with transmitted polarized lights and a digital Canon camera.

To test the specificity of the sensor it was exposed to a mix of β-lactoglobulin and a random protein, in this case ovalbumin. The results can be seen on Figure 32 below. Bases on previous results from this work it was expected that the image would be bright since that is the response obtained when the liquid crystal is subjected to the aptamer-amphiphile and subsequently to the target protein. The bright image obtained, Figure 32, corroborates with the hypothesis that the sensor developed is specific.

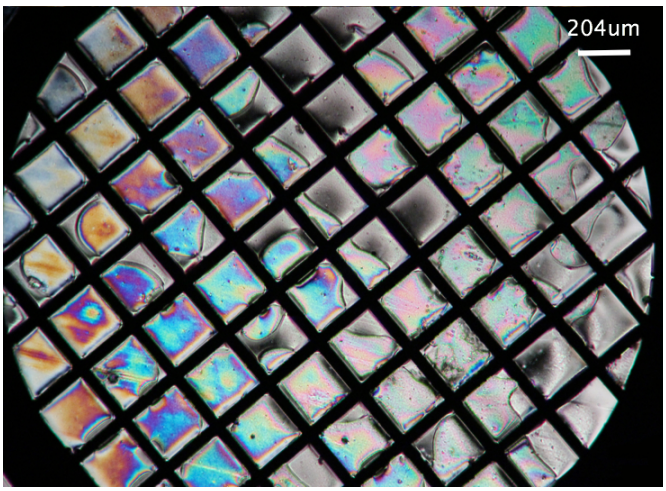

Figure 32 Optical images of the 5CB LC confined to a copper grid supported on a OTS treated glass under the polarizing microscope. The images reflect the LC exposed to the aptamer-amphiphile and subsequently to a mix of 10μM ovalbumin solution and a 10μM β-lactoglobulin. The image was obtained using a Nikon microscope with transmitted polarized lights and a digital Canon camera.

5. Conclusions

Food allergies are an increasing concern; every year it is estimated that about 30,000 Americans visits the emergency room to get treatment because of allergic reactions. It is estimated also that every year about 150 to 200 Americans dies due to severe food related allergic reactions (FDA 2009). Milk and milk ingredients are the most prevalent allergy among young kids. It is known that 90% of all food allergies are caused by 8 foods and milk is one of them (Sampson 2004).

Food allergies also have a huge economic impact. A food containing an undeclared allergen is considered adulterated and misbranded and the company must recall the product. The number one cause of food recalls in the United Stated is due to undeclared allergens. It is estimated that the direct cost of a food recall can cost the company up to $10 million dollars (Tyco Integrated Security 2012; Maberry 2015).

Among all milk proteins β-lactoglobulin, a major component of whey proteins, is identified as being the more allergenic among all milk proteins. Considering the potential problem of undeclared allergens in food products showed the need for the development of a method that could selectively detect specific allergens, in this work β-lactoglobulin, mainly on plant surfaces. The pair

aptamer-amphiphile and liquid crystal were the materials of choice for the development of the sensor.

Aptamers are a single strained DNA material that specifically binds to selected targets (Famulok et al. 2000). They are being recognized as a flexible substance and has some advantages in comparison to antibodies used in ELISA tests, aptamers are less expensive, the selection process is totally in vitro, and are designated to target almost any molecule, it is stable at room temperature, and can withstand some mild temperature elevation, and can be easily modified (Toh et al. 2015). Aptamers-amphiphile is one of those modifications that has gained attention lately. This molecule is composed of a ssDNA head group and a hydrocarbon tail (Pearce et al. 2014).

Liquid crystals are substances being largely used for sensing techniques. It has a unique characteristic, the ability to easily be aligned with the contact surface, the liquid crystal will order itself in accordance with the chemistry and geometry of the surface (Nazarenko and Nych 1999). Exploring this property, the work proposed in this thesis were developed. A sensor that combines liquid crystal material and aptamer-amphiphiles aiming to detect β-lactoglobulin.

An aptamer sequence from the literature was tested to determine the binding affinity to the target protein, β-lactoglobulin. The K_d= 2.88 ± 0.056 nM was obtained indicating that the sequence selected has a high affinity to the target protein. In addition, three ssDNA amphiphiles were synthesized and

evaluated in regards to its binding affinity. The three ssDNA amphiphiles synthesized were the C12, T10, and the NoSPR. The name of those indicates how the molecule was synthesized, C12 mean that 12 carbons were inserted between the DNA head group and the carbonic tail, T10 mean that 10 thymine molecules were inserted between the DNA head group and the tail, and also a ssDNA amphiphile that the DNA head group was hybridized directly to the carbonic tail, NoSPR.

The binding constants for the three amphiphiles were; C12 K_d= 134 $\pm$ 7.937 nM, T10 K_d= 127 $\pm$ 4.58 nM, and NoSPR K_d= 45 $\pm$ 1.68 nM. Observing the values obtained it was possible to conclude that the NoSPR amphiphile has the highest affinity to the target, and the smallest K_d, so that was the amphiphile of choice to be used on the sensor.

The sensor was assembled using a glass slide, cleaned with piranha solution, a TEM copper grid and the liquid crystal confined within the grid. The liquid crystal sensor was them exposed to different environments (air, water and SDS) and subsequently analyzed under the polarizing microscope. As it shows in Figure 29 the images obtained are in accordance with what was published in the literature for this type of assembly, a dark image was visualized when the liquid crystal was exposed to air and water and a bright image was obtained when it was exposed to a surfactant (Brake and Abbott 2002a).

The sensor was then exposed to the aptamer-amphiphile and the image was visualized under the polarizing microscope and subsequently the sensor was exposed to a target protein. As it was hypothesized the image obtained was dark when the sensor was exposed only to the aptamer-amphiphile, once the target was introduced the image changed to bright, as shown in Figure 29. To further evaluate the sensor the limit of detection was obtained as being 0.01μM, 18.4 ng, or 1.84 ppm. Even though this limit of detection is slight higher than commercial available ELISA methods, the method developed in this work is much easier and fast to perform and it targets surfaces testing differently than the commercial available methods for β-lactoglobulin. The majority of those methods are developed to test food products.

In conclusion, this work was able to confirm the hypothesis that a system comprised of liquid crystal and an aptamer-amphiphile that has an affinity to the target protein can potentially be used as a sensing technique to detect allergenic proteins. The findings of this work is a first step for potentially what can be a cheap, quick and reliable technique. In the future, specific aptamers can be developed for the desired target proteins and a more automated sensor assembly can be idealized for application in food processing plants.

6. References

Alvarez P a., Boye JI (2012) Food Production and Processing Considerations of Allergenic Food Ingredients: A Review. J Allergy 2012:1–14. doi: 10.1155/2012/746125

Amaya-González S, De-los-Santos-Álvarez N, Miranda-Ordieres AJ, Lobo-Castañón MJ (2015) Sensitive gluten determination in gluten-free foods by an electrochemical aptamer-based assay. Anal Bioanal Chem 6021–6029. doi: 10.1007/s00216-015-8771-6

Aquino-Jarquin G, Toscano-Garibay JD (2011) RNA aptamer evolution: Two decades of selection. Int J Mol Sci 12:9155–9171. doi: 10.3390/ijms12129155

Biocompare.com ELISA Kit for Beta-Lactoglobulin (bLg) EKU02707 from Biomatik |. http://www.biocompare.com/9956-Assay-Kit/5820815-ELISA-Kit-for-Beta-Lactoglobulin-bLg/?vpim=1&soids=2&ppim=5820815_0_1&ncatid=9956&dfp=true. Accessed 25 May 2016

Brake JM, Abbott NL (2002a) An Experimental System for Imaging the Reversible Adsorption of Amphiphiles at Aqueous−Liquid Crystal Interfaces. Langmuir 18:6101–6109. doi: 10.1021/la011746t

Brake JM, Abbott NL (2002b) An experimental system for imaging the reversible adsorption of amphiphiles at aqueous-liquid crystal interfaces. Langmuir 18:6101–6109. doi: 10.1021/la011746t

Branum AM, Lukacs SL (2008) Food allergy among U.S. children: trends in prevalence and hospitalizations. NCHS Data Brief 1–8.

Brownlow S, Cabral JHM, Cooper R, et al (1997) Bovine β-lactoglobulin at 1.8 Å resolution — still an enigmatic lipocalin. Structure 5:481–495. doi: 10.1016/S0969-2126(97)00205-0

Bruno JG, Carrillo MP, Phillips T, Andrews CJ (2010) A novel screening method for competitive FRET-aptamers applied to E. coli assay development. J Fluoresc 20:1211–1223. doi: 10.1007/s10895-010-0670-9

Bryan TM, Baumann P (2010) G-Quadruplexes: From Guanine Gels to Chemotherapeutics. In: Baumann P (ed) G-Quadruplex DNA. Humana Press, pp 1–10

Busch MHA, Carels LB, Boelens HFM, et al (1997) Comparison of five methods for the study of drug–protein binding in affinity capillary electrophoresis. J Chromatogr A 777:311–328. doi: 10.1016/S0021-9673(97)00369-5

Center for Food Safety and Applied Nutrition (2006) Allergens - Guidance for Industry: Questions and Answers Regarding Food Allergens, including the Food Allergen Labeling and Consumer Protection Act of 2004 (Edition 4); Final Guidance.

Centers for Disease Control and Prevention (2011) CDC Estimates of Foodborne Illness in the United States CDC 2011. 68:3–4. doi: 10.1111/j.1753-4887.2010.00286.x
Chen H, Gao J (2012) Food Allergen Epitopes. Multidisciplinary Approaches to Allergies.
Cho EJ, Lee J-W, Ellington AD (2009) Applications of aptamers as sensors. Annu Rev Anal Chem (Palo Alto Calif) 2:241–264. doi: 10.1146/annurev.anchem.1.031207.112851
Craig JA, Rexeisen EL, Mardilovich A, et al (2008) Effect of linker and spacer on the design of a fibronectin-mimetic peptide evaluated via cell studies and AFM adhesion forces. Langmuir 24:10282–10292. doi: 10.1021/la702434p
Crystal Chem Beta-lactoglobulin ELISA Kits, Milk Allergen Kit |. http://www.crystalchem.com/beta-lactoglobulin-elisa-kit.html. Accessed 25 May 2016
Dong Y, Xu Y, Yong W, et al (2014) Aptamer and its potential applications for food safety. Crit Rev Food Sci Nutr 54:1548–61. doi: 10.1080/10408398.2011.642905
Ehn B-M, Ekstrand B, Bengtsson U, Ahlstedt S (2004) Modification of IgE binding during heat processing of the cow's milk allergen beta-lactoglobulin. J Agric Food Chem 52:1398–1403. doi: 10.1021/jf0304371
Ellington AD, Szostak JW (1990) In vitro selection of RNA molecules that bind specific ligands. Nature 346:818–22. doi: 10.1038/346818a0
ExpertRECALL S (2011) ExpertRECALL Quarterly Recall Index.
Famulok M, Mayer G, Blind M (2000) Nucleic acid aptamers - From selection in vitro to applications in vivo. Acc Chem Res 33:591–599. doi: 10.1021/ar960167q
Farrell HM, Jimenez-Flores R, Bleck GT, et al (2004) Nomenclature of the Proteins of Cows' Milk—Sixth Revision. J Dairy Sci 87:1641–1674. doi: 10.3168/jds.S0022-0302(04)73319-6
FDA (2009) Food Allergies : Reducing the Risks. FDA Consum Heal Inf 1–2.
GELLERT M, LIPSETT MN, DAVIES DR (1962) Helix formation by guanylic acid. Proc Natl Acad Sci U S A 48:2013–8.
Girardot M, Li H, Descroix S, Varenne A (2013) Aptamer–Target Interaction: A Comprehensive Study by Microchip Electrophoresis in Frontal Mode. Chromatographia 76:305–312. doi: 10.1007/s10337-012-2346-x
Girardot M, Li H-Y, Descroix S, Varenne A (2011) Determination of binding parameters between lysozyme and its aptamer by frontal analysis continuous microchip electrophoresis (FACMCE). J Chromatogr A 1218:4052–4058. doi: 10.1016/j.chroma.2011.04.077
Goff HD, Hill HD (1992) Dairy Science and Technology Handbook 1 Principles and Properties. In: Hui YH (ed)WILEY-VCH, Inc., p 2=62
Iglesias W, Abbott NL, Mann EK, Jakli A (2012) Improving Liquid-Crystal-Based

Biosensing in Aqueous Phases. Appl Mater Interfacesaterials Interfaces 2:6884–6890.
Immer U, Lacorn M (2015) Enzyme-linked immunosorbent assays (ELISAs) for detecting allergens in food. Handbook of Food Allergen Detection and Control. Elsevier, pp 199–217
Jayasena SD (1999) Aptamers: An emerging class of molecules that rival antibodies in diagnostics. Clin Chem 45:1628–1650.
Jerome B (1999) Surface effects and anchoring in liquid crystals. Reports Prog Phys 54:391–451. doi: 10.1088/0034-4885/54/3/002
Jing, Meng and Bowser MT (2012) A Review of Methods for Measuring Aptamer-Protein Equilibria. 686:9–18. doi: 10.1016
Kypr J, Kejnovska I, Renciuk D, Vorlickova M (2009) Circular dichroism and conformational polymorphism of DNA. Nucleic Acids Res 37:1713–1725. doi: 10.1093/nar/gkp026
Lamont E a, He L, Warriner K, et al (2011) A single DNA aptamer functions as a biosensor for ricin. Analyst 136:3884–3895. doi: 10.1039/c1an15352h
Lockwood N, Gupta J, Abbott N (2008) Self-assembly of amphiphiles, polymers and proteins at interfaces between thermotropic liquid crystals and aqueous phases. Surf Sci Rep 63:255–293. doi: 10.1016/j.surfrep.2008.02.002
Luo K, Bu G (2012) Cow ' s Milk Allergens and Technologies to Control Allergenicity. Multidisciplinary Approaches to Allergies.
Luzi E, Minunni M, Tombelli S, Mascini M (2003) New trends in affinity sensing. TrAC Trends Anal Chem 22:810–818. doi: 10.1016/S0165-9936(03)01208-1
Maberry T (2015) Q3 Food Recalls: Undeclared Allergens Still Dominate - Food Safety Magazine. Food Saf. Mag.
Mcgown LB, Rehder MA (2001) Open-tubular capillary electrochromatography of bovine â -lactoglobulin variants A and B using an aptamer stationary phase. Electrophoresis 22:3759–3764.
McSweeney PLH, Fox PF (2009) Advanced dairy chemistry.
McUmber AC, Noonan PS, Schwartz DK (2012) Surfactant–DNA interactions at the liquid crystal–aqueous interface. Soft Matter 8:4335. doi: 10.1039/c2sm07483d
Mendonsa SD, Bowser MT (2004) In vitro evolution of functional DNA using capillary electrophoresis. J Am Chem Soc 126:20–21. doi: 10.1021/ja037832s
National Institute of Allergy and Infectious Diseases (2012) Food Allergy An Overview. 7540. doi: 10.1016/j.jaci.2010.10.008
Nazarenko V, Nych a (1999) Multistable alignment in free suspended nematic liquid crystal films. Phys Rev E Stat Phys Plasmas Fluids Relat Interdiscip Topics 60:R3495–7.
Noonan PS, Roberts RH, Schwartz DK (2013) Liquid crystal reorientation induced by aptamer conformational changes. J Am Chem Soc 135:5183–9.

doi: 10.1021/ja400619k
Nutrition C for FS and A Allergens - Food Allergen Labeling and Consumer Protection Act of 2004 (Public Law 108-282, Title II).
Nutrition C for FS and A Food Safety Modernization Act (FSMA) - Full Text of the Food Safety Modernization Act (FSMA).
Obenauer JC, Yaffe MB (2004) Computational prediction of protein-protein interactions.
Ohk SH, Koo OK, Sen T, et al (2010) Antibody-aptamer functionalized fibre-optic biosensor for specific detection of Listeria monocytogenes from food. J Appl Microbiol 109:808–817. doi: 10.1111/j.1365-2672.2010.04709.x
Pearce TR (2014) Self-assembly of ssDNA-amphiphiles into micelles , nanotapes and nanotubes. University of Minnesota
Pearce TR, Kokkoli E (2013) Supplementary Information amphiphiles into micelles and nanotapes.
Pearce TR, Kokkoli E (2015) DNA nanotubes and helical nanotapes via self-assembly of ssDNA-amphiphiles. Soft Matter 11:109–117. doi: 10.1039/C4SM01332H
Pearce TR, Waybrant B, Kokkoli E (2014) The role of spacers on the self-assembly of DNA aptamer-amphiphiles into micelles and nanotapes. Chem Commun Chem Commun 210:210–212. doi: 10.1039/c3cc42311e
S.C. W, Davis PJ (1998) Protein modification by thermal processing. Allergy 53:102–105. doi: 10.1111/j.1398-9995.1998.tb04975.x
Sampson HA (2004) Update on food allergy. J Allergy Clin Immunol 113:805–819. doi: 10.1016/j.jaci.2004.03.014
Shroff K, Pearce TR, Kokkoli E (2012) Enhanced integrin mediated signaling and cell cycle progression on fibronectin mimetic peptide amphiphile monolayers. Langmuir 28:1858–1865. doi: 10.1021/la203322t
Swiss Re (2015) Number of food recalls and their costs are rising | Swiss Re - Leading Global Reinsurer.
Taylor SL, Gendel SM, Houben GF, Julien E (2009) The Key Events Dose-Response Framework: a foundation for examining variability in elicitation thresholds for food allergens. Crit Rev Food Sci Nutr 49:729–39. doi: 10.1080/10408390903098707
Taylor SL, Hefle SL, Bindslev-Jensen C, et al (2004) Factors affecting the determination of threshold doses for allergenic foods: How much is too much? J Allergy Clin Immunol 34:689–695. doi: 10.1111/j.1365-2222.2004.1886.x
Taylor SL, Hourihabe JO, Baumert JL (2013) Food Allergen Thresholds of Reactivity. In: Metcalfe DD, Sampson HA, Simon RA, Lack G (eds) Food Allergy: Adverse Reactions to Foods and Food Additives, 5th edn. John Wiley & Sons Ltd, Chichester, UK, pp 90–99
Toh SY, Citartan M, Gopinath SCB, Tang T-H (2015) Aptamers as a replacement

for antibodies in enzyme-linked immunosorbent assay. Biosens Bioelectron 64:392–403. doi: 10.1016/j.bios.2014.09.026
Tran DT, Knez K, Janssen KP, et al (2013) Selection of aptamers against Ara h 1 protein for FO-SPR biosensing of peanut allergens in food matrices. Biosens Bioelectron 43:245–251. doi: 10.1016/j.bios.2012.12.022
Tuerk C, Larry G (1990) Systematic Evolution of Ligands by Exponential Enrichment : RNA Ligands to Bacteriophage T4 DNA Polymerase. Science (80-) 249:505–510.
Tyco Integrated Security (2012) Recall : The Food Industry's Biggest Threat to Profitability.
Walstra P, Wouters JTM, Geurts TJ (2006) Dairy Science and Technology, 2nd edn. CRC Press Taylor & Francis Group, Boca Raton
Waybrant B, Pearce TR, Kokkoli E (2014) Effect of Polyethylene Glycol, Alkyl, and Oligonucleotide Spacers on the Binding, Secondary Structure, and Self-Assembly of Fractalkine Binding FKN-S2 Aptamer-Amphiphiles.
Woody RW (1995) Circular dichroism. Methods Enzymol 246:34–71. doi: 10.1016/0076-6879(95)46006-3
Zhang J, Zhang B, Wu Y, et al (2010) Fast determination of the tetracyclines in milk samples by the aptamer biosensor. Analyst 135:2706–2710. doi: 10.1039/c0an00237b
(1906) 21 USC Ch. 1: Adulterated or Misbranded Foods or Drugs From Title 21-Food and Drugs.
(2016) 21 USC 342: Adulterated food From Tittle 21- Food and Drugs.

Appendices

Appendix A- Capillary Electrophoresis (CE) binding evaluation.

This part reflects the first attempted to evaluate the binding of the aptamer and β-lactoglobulin.

Materials

β-lactoglobulin (Davisco Foods International, Eden Prairie, MN, DNA aptamer 5'-GGG GTT GGG GTG TGG GGT TGG GG-3' (Integrated DNA Technologies, Coralville, IA), sodium chloride crystal (NaCl) (Macron Fine Chemicals, Center Valley, PA), nuclease free water (Integrated DNA Technologies, Coralville, IA), sodium hydroxide (NaOH) 1N solution (Fisher Chemical, Hanover Park, IL), P/ACE MDQ Capillary Electrophoresis System (Beckman Coulter, Furllerton, CA).

Methods

DNA aptamer samples were prepared in 10 mM NaCl in nuclease free water, concentrations 10, 15, 20, 25, 30 μM. The β-lactoglobulin solution, stock 100 μM, was prepared in nuclease free water. The protein solution was then added to each aptamer concentration for the final concentration of 10 μM, the samples were incubated at room temperature for at least 20 min. The capillary

electrophoresis was performed using an uncoated fused silica capillary that was 40 cm long (detection window at 30cm), with an inner diameter of 50 μm and 360 μm outer diameter on the P/ACE MDQ Capillary Electrophoresis System. The procedure started with a capillary conditioning, rinse with NaOH 1 M for 10 min at 20 psi pressure. The capillary was then filled with the incubation buffer, 10 mM NaCl, for 5 minutes with 20 psi 15 kV voltage. The sample was then injected by pressure, 5 psi for 4 secods. The separation was performed applying a positive 15 kV for 10 minutes, in the incubation buffer and the progress was monitored by UV absorbance at 254 nm. In between each sample the capillary was rinsed for 5 min with 0.1 M NaOH at 20 psi and 5 min with nuclease free water also at 20 psi. To finalize the capillary was again rinsed with 1 M NaOH at 20 psi for 10 min. All the samples utilized in the CE were sonicated prior to use to avoid gas in the vial. This procedure was done in triplicate for each concentration and the results were averaged.

Results and Discussion

The binding study performed using capillary electrophoresis was performed in the frontal mode (FA), the capillary is first filled with buffer then the sample is injected, it was based on the Girardot et. al. (2011) work. There are two immediate results obtained with this technique, the UV spectrum (Figure 33,

34,35) and the plateau height from that spectrum that will be used to calculate the Kd (Figure 36, Table 5).

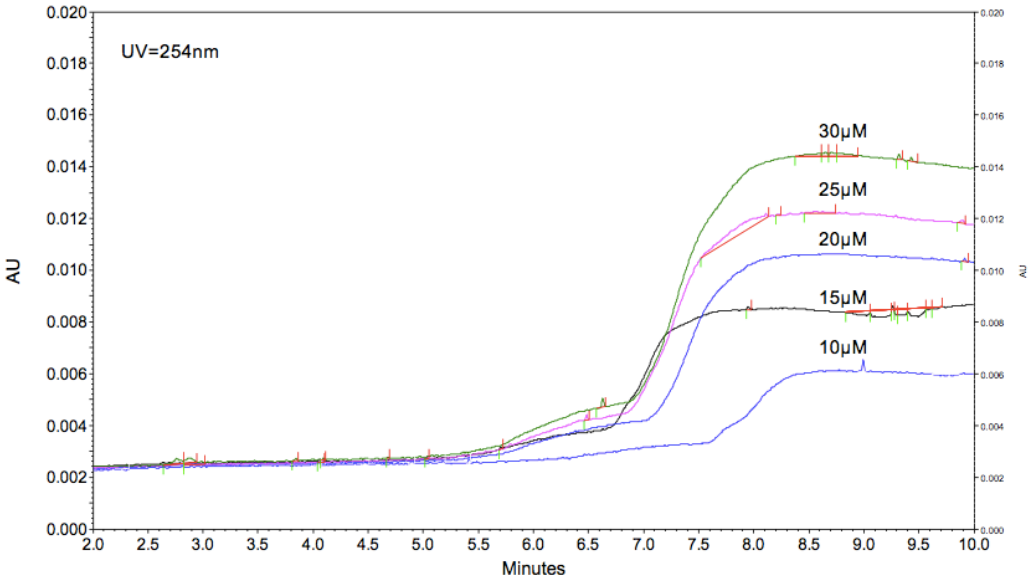

Figure 33 UV, 254nM, electropherogram obtain from the capillary electrophoresis binding study, each plateau height represents a fixed protein concentration10µM, and variable aptamer concentration, 10, 15, 20, 25 and 30 µM.

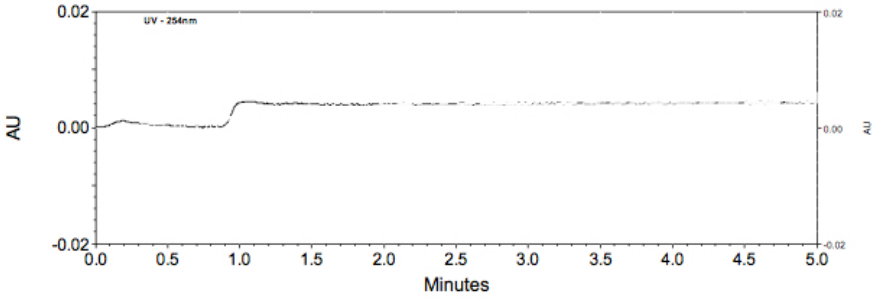

Figure 34 Electropherogram 10µM aptamer in 10mM NaCl.

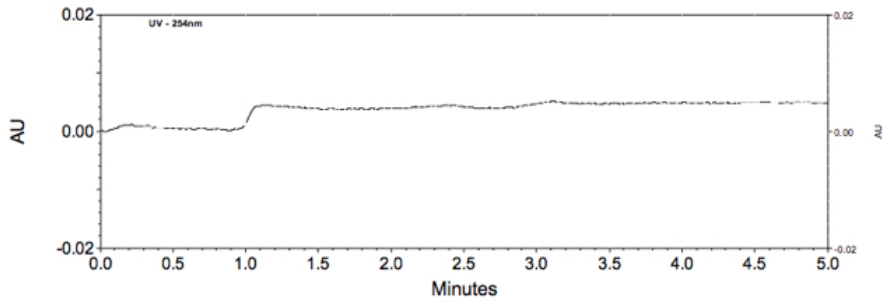

Figure 35 Electropherogram of a 10μM β-lactoglobulin solution

When using the FA mode it is necessary to make some assumptions such as the mobility of the free aptamer and the complex are significantly different (Busch et al. 1997). In the Figure 34 it is possible to notice that the free aptamer does not reach the detector using the same conditions as for the complex, Figure 33, this is also true for the protein solution, Figure 35. A possible explanation for this is that DNA is usually negatively charged at a pH around 6.5 (pH of the binding buffer, 10mM NaCl) due to phosphate groups deprotonation. β-lactoglobulin has its isoelectric point at pH 5.1, so it also would be negatively charged at pH 6.5. For the CE separation, a positive voltage was applied, the detection window was in the cathodic electrode, so neither the DNA nor the protein travel through the capillary. Using the same assumptions, it is possible to conclude that the plateaus observed in Figure 33, are a representation of the aptamer-protein complex.

Table 5 Triplicate measurement of for the complex plateau height obtained from the CE binding study, and its respective average and standard deviation.

Aptamer concentration (μM)	Plateau Height			Average	SD
10	0.0059	0.0057	0.0058	0.0058	0.0001
15	0.0085	0.0076	0.0082	0.0081	0.0005
20	0.0106	0.0103	0.0102	0.0103	0.0002
25	0.0122	0.0112	0.0132	0.0125	0.0005
30	0.0144	0.0146	00147	0.0145	0.0002

The plateaus heights, Table 5, were obtained from the electropherogram for the complex, the data was averaged and plotted against the aptamer concentration, Figure 36. It is possible to notice that the relation between amplitude and aptamer concentration is linear, r^2=0.9995, so using the same equation proposed by Girardot et al. (2013), equation (1), the K_d was obtained from the linear fit equation as being 2.2 nM what indicates a very good binding, low K_d means low possibility of the complex to dissociate, high affinity.

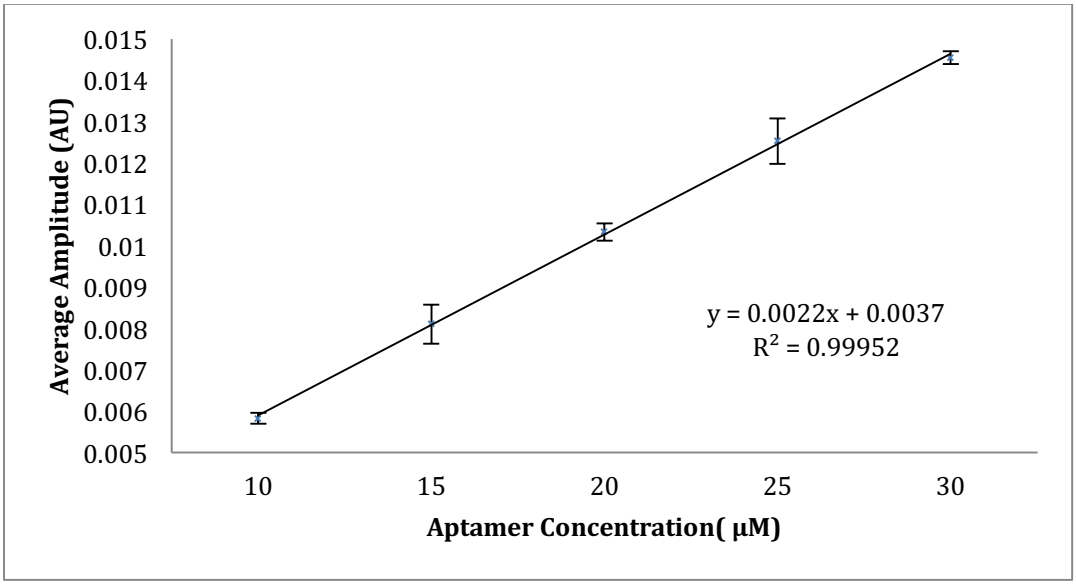

Figure 36 Plot of the average plateau heights (AU) versus aptamer concentration (μM)

Appendix B- Tables results used to calculate the K_d and plot the curves presented on the evaluation of binding constant result section (4.2)

Aptamer 5'-/5Bioseg/-GGG GTT GGG GTG TGG GGT TGG GG-3' + β lactoglobulin

Table 6 Values collected from UV-Vis measurement during the ELISA procedure for the calculation of the K_d for the aptamer.

Aptamer Concentration	Absorbance Replicates			Average	SD
	1	2	3		
0	0.068	0.067	0.056	0.0637	0.0067
0.01	0.064	0.066	0.067	0.0657	0.0015
0.1	0.059	0.063	0.078	0.0667	0.0100
0.5	0.099	0.077	0.068	0.0813	0.0159
1	0.088	0.108	0.096	0.0973	0.0101
5	0.112	0.107	0.108	0.1090	0.0026
10	0.615	0.606	0.657	0.6260	0.0272
50	1.755	1.789	1.744	1.7627	0.0235
100	2.359	2.393	2.367	2.3730	0.0178
1000	2.542	2.526	2.497	2.5217	0.0228
5000	2.555	2.547	2.66	2.5873	0.0631
10000	2.611	2.553	2.613	2.5923	0.0341
20000	2.571	2.631	2.618	2.6067	0.0316
30000	2.647	2.588	2.608	2.6143	0.0300
K_d	2.92	2.81	2.88	2.88nM	0.0557
Bmax	2.58	2.56	2.6	2.58	0.02

Table 7 Calculated values using Equation 3 for the curve fit for the aptamer, from Figure18.

Fit			
Assumed Aptamer Concertation	**Absorbance**	**Assumed Aptamer Concentration**	**Absorbance**
1.00E-04	0.0022	**1.92E+00**	0.1639
1.22E-04	0.0022	**2.34E+00**	0.1966
1.48E-04	0.0022	**2.85E+00**	0.2351
1.81E-04	0.0022	**3.47E+00**	0.2803
2.20E-04	0.0022	**4.22E+00**	0.3327
2.68E-04	0.0023	**5.14E+00**	0.3938
3.27E-04	0.0023	**6.26E+00**	0.4638
3.98E-04	0.0023	**7.63E+00**	0.5436
4.84E-04	0.0023	**9.29E+00**	0.6326
5.90E-04	0.0023	**1.13E+01**	0.7305
7.19E-04	0.0023	**1.38E+01**	0.8392
8.75E-04	0.0023	**1.68E+01**	0.9540
1.07E-03	0.0023	**2.05E+01**	1.0763
1.30E-03	0.0023	**2.49E+01**	1.1997
1.58E-03	0.0024	**3.03E+01**	1.3261
1.93E-03	0.0024	**3.70E+01**	1.4539
2.35E-03	0.0024	**4.50E+01**	1.5762
2.86E-03	0.0025	**5.48E+01**	1.6940
3.48E-03	0.0025	**6.68E+01**	1.8053
4.24E-03	0.0026	**8.13E+01**	1.9074
5.17E-03	0.0027	**9.91E+01**	2.0011
6.29E-03	0.0028	**1.21E+02**	2.0858
7.66E-03	0.0029	**1.47E+02**	2.1589
9.33E-03	0.0031	**1.79E+02**	2.2238
1.14E-02	0.0033	**2.18E+02**	2.2801
1.38E-02	0.0035	**2.66E+02**	2.3290
1.69E-02	0.0037	**3.24E+02**	2.3702
2.05E-02	0.0041	**3.94E+02**	2.4050
2.50E-02	0.0045	**4.80E+02**	2.4346
3.05E-02	0.0050	**5.85E+02**	2.4594
3.71E-02	0.0056	**7.12E+02**	2.4801
4.52E-02	0.0063	**8.67E+02**	2.4974
5.51E-02	0.0072	**1.06E+03**	2.5120
6.71E-02	0.0082	**1.29E+03**	2.5239
8.17E-02	0.0095	**1.57E+03**	2.5337

9.95E-02	0.0111	**1.91E+03**	2.5418
1.21E-01	0.0131	**2.33E+03**	2.5486
1.48E-01	0.0155	**2.83E+03**	2.5541
1.80E-01	0.0183	**3.45E+03**	2.5587
2.19E-01	0.0218	**4.20E+03**	2.5625
2.67E-01	0.0260	**5.12E+03**	2.5656
3.25E-01	0.0311	**6.23E+03**	2.5682
3.96E-01	0.0373	**7.59E+03**	2.5703
4.82E-01	0.0448	**9.25E+03**	2.5720
5.87E-01	0.0539	**1.13E+04**	2.5735
7.15E-01	0.0649	**1.37E+04**	2.5746
8.71E-01	0.0782	**1.67E+04**	2.5756
1.06E+00	0.0940	**2.04E+04**	2.5764
1.29E+00	0.1131	**2.48E+04**	2.5770
1.57E+00	0.1359	**3.02E+04**	2.5776

Aptamer 5'-/5Biosg/ TTT TTT TTT TTT TTT TTT TTT TT-3' + β lactoglobulin.

Table 8 Values collected from UV-Vis measurement during the ELISA procedure for the calculation of the K_d for the random aptamer.

Aptamer Concentration	Absorbance Replicates			Average	SD
	1	2	3		
0	0.026	0.036	0.039	0.034	0.007
0.01	0.029	0.036	0.036	0.034	0.004
0.1	0.035	0.034	0.035	0.035	0.001
0.5	0.033	0.037	0.037	0.036	0.002
1	0.033	0.036	0.037	0.035	0.002
5	0.04	0.031	0.037	0.036	0.005
10	0.039	0.043	0.039	0.040	0.002
50	0.128	0.127	0.128	0.128	0.001
100	0.262	0.266	0.272	0.267	0.005
1000	0.598	0.62	0.607	0.608	0.011
5000	0.702	0.745	0.724	0.724	0.022
10000	0.74	0.727	0.746	0.738	0.010
20000	0.733	0.742	0.75	0.742	0.009
30000	0.753	0.732	0.747	0.744	0.011
K_d	242	241	254	246nM	7.234
Bmax	0.721	0.717	0.719	0.719	0.002

Table 9 Calculated values using Equation 3 for the curve fit for the randon aptamer sequence, from Figure 19.

Fit			
Assumed Aptamer Concertation	**Absorbance**	**Assumed Aptamer Concentration**	**Absorbance**
1.00E-04	0.0002	**1.92E+00**	0.0059
1.22E-04	0.0002	**2.34E+00**	0.0071
1.48E-04	0.0002	**2.85E+00**	0.0086
1.81E-04	0.0002	**3.47E+00**	0.0104
2.20E-04	0.0002	**4.22E+00**	0.0126
2.68E-04	0.0002	**5.14E+00**	0.0152
3.27E-04	0.0002	**6.26E+00**	0.0184
3.98E-04	0.0002	**7.63E+00**	0.0223
4.84E-04	0.0002	**9.29E+00**	0.0269
5.90E-04	0.0002	**1.13E+01**	0.0325
7.19E-04	0.0002	**1.38E+01**	0.0392
8.75E-04	0.0002	**1.68E+01**	0.0472
1.07E-03	0.0002	**2.05E+01**	0.0568
1.30E-03	0.0002	**2.49E+01**	0.0678
1.58E-03	0.0002	**3.03E+01**	0.0809
1.93E-03	0.0002	**3.70E+01**	0.0965
2.35E-03	0.0002	**4.50E+01**	0.1142
2.86E-03	0.0002	**5.48E+01**	0.1346
3.48E-03	0.0002	**6.68E+01**	0.1579
4.24E-03	0.0002	**8.13E+01**	0.1839
5.17E-03	0.0002	**9.91E+01**	0.2129
6.29E-03	0.0002	**1.21E+02**	0.2447
7.66E-03	0.0002	**1.47E+02**	0.2780
9.33E-03	0.0002	**1.79E+02**	0.3136
1.14E-02	0.0003	**2.18E+02**	0.3504
1.38E-02	0.0003	**2.66E+02**	0.3881
1.69E-02	0.0003	**3.24E+02**	0.4254
2.05E-02	0.0003	**3.94E+02**	0.4615
2.50E-02	0.0003	**4.80E+02**	0.4964
3.05E-02	0.0003	**5.85E+02**	0.5294
3.71E-02	0.0003	**7.12E+02**	0.5596
4.52E-02	0.0004	**8.67E+02**	0.5873
5.51E-02	0.0004	**1.06E+03**	0.6127
6.71E-02	0.0004	**1.29E+03**	0.6346
8.17E-02	0.0005	**1.57E+03**	0.6538

9.95E-02	0.0005	**1.91E+03**	0.6705
1.21E-01	0.0006	**2.33E+03**	0.6851
1.48E-01	0.0007	**2.83E+03**	0.6972
1.80E-01	0.0008	**3.45E+03**	0.7077
2.19E-01	0.0009	**4.20E+03**	0.7165
2.67E-01	0.0010	**5.12E+03**	0.7240
3.25E-01	0.0012	**6.23E+03**	0.7301
3.96E-01	0.0014	**7.59E+03**	0.7353
4.82E-01	0.0017	**9.25E+03**	0.7396
5.87E-01	0.0020	**1.13E+04**	0.7432
7.15E-01	0.0023	**1.37E+04**	0.7461
8.71E-01	0.0028	**1.67E+04**	0.7486
1.06E+00	0.0034	**2.04E+04**	0.7506
1.29E+00	0.0040	**2.48E+04**	0.7523
1.57E+00	0.0049	**3.02E+04**	0.7536

Aptamer 5'-/5Bioseg/-GGG GTT GGG GTG TGG GGT TGG GG-3' + α lactalbumin

Table 10 Values collected from UV-Vis measurement during the ELISA procedure for the calculation of the K_d for the aptamer and α-lactalbumin.

Aptamer Concentration	Absorbance Replicates			Average	SD
	1	2	3		
0	0.013	0.01	0.008	0.0103	0.0025
0.01	0.013	0.015	0.017	0.0150	0.0020
0.1	0.016	0.014	0.015	0.0150	0.0010
0.5	0.016	0.016	0.014	0.0153	0.0012
1	0.016	0.013	0.017	0.0153	0.0021
5	0.015	0.016	0.016	0.0157	0.0006
10	0.029	0.028	0.022	0.0263	0.0038
50	0.135	0.137	0.134	0.1353	0.0015
100	0.2	0.204	0.207	0.2037	0.0035
1000	0.612	0.605	0.631	0.6160	0.0135
5000	0.735	0.711	0.712	0.7193	0.0136
10000	0.731	0.72	0.751	0.7340	0.0157
20000	0.736	0.726	0.754	0.7387	0.0142
30000	0.76	0.709	0.754	0.7410	0.0279
K_d	274	248	257	259 nM	13.2035
Bmax	0.738	0.725	0.756	0.7430	0.0156

Table 11 Calculated values using Equation 3 for the curve fit for the aptamer with α-lactalbumin, from Figure 20.

Fit			
Assumed Aptamer Concertation	**Absorbance**	**Assumed Aptamer Concentration**	**Absorbance**
1.00E-04	0.0002	**1.92E+00**	0.0059
1.22E-04	0.0002	**2.34E+00**	0.0071
1.48E-04	0.0002	**2.85E+00**	0.0086
1.81E-04	0.0002	**3.47E+00**	0.0104
2.20E-04	0.0002	**4.22E+00**	0.0126
2.68E-04	0.0002	**5.14E+00**	0.0152
3.27E-04	0.0002	**6.26E+00**	0.0184
3.98E-04	0.0002	**7.63E+00**	0.0223
4.84E-04	0.0002	**9.29E+00**	0.0269
5.90E-04	0.0002	**1.13E+01**	0.0325
7.19E-04	0.0002	**1.38E+01**	0.0392
8.75E-04	0.0002	**1.68E+01**	0.0472
1.07E-03	0.0002	**2.05E+01**	0.0568
1.30E-03	0.0002	**2.49E+01**	0.0678
1.58E-03	0.0002	**3.03E+01**	0.0809
1.93E-03	0.0002	**3.70E+01**	0.0965
2.35E-03	0.0002	**4.50E+01**	0.1142
2.86E-03	0.0002	**5.48E+01**	0.1346
3.48E-03	0.0002	**6.68E+01**	0.1579
4.24E-03	0.0002	**8.13E+01**	0.1839
5.17E-03	0.0002	**9.91E+01**	0.2129
6.29E-03	0.0002	**1.21E+02**	0.2447
7.66E-03	0.0002	**1.47E+02**	0.2780
9.33E-03	0.0002	**1.79E+02**	0.3136
1.14E-02	0.0003	**2.18E+02**	0.3504
1.38E-02	0.0003	**2.66E+02**	0.3881
1.69E-02	0.0003	**3.24E+02**	0.4254
2.05E-02	0.0003	**3.94E+02**	0.4615
2.50E-02	0.0003	**4.80E+02**	0.4964
3.05E-02	0.0003	**5.85E+02**	0.5294
3.71E-02	0.0003	**7.12E+02**	0.5596
4.52E-02	0.0004	**8.67E+02**	0.5873
5.51E-02	0.0004	**1.06E+03**	0.6127
6.71E-02	0.0004	**1.29E+03**	0.6346
8.17E-02	0.0005	**1.57E+03**	0.6538

9.95E-02	0.0005	**1.91E+03**	0.6705
1.21E-01	0.0006	**2.33E+03**	0.6851
1.48E-01	0.0007	**2.83E+03**	0.6972
1.80E-01	0.0008	**3.45E+03**	0.7077
2.19E-01	0.0009	**4.20E+03**	0.7165
2.67E-01	0.0010	**5.12E+03**	0.7240
3.25E-01	0.0012	**6.23E+03**	0.7301
3.96E-01	0.0014	**7.59E+03**	0.7353
4.82E-01	0.0017	**9.25E+03**	0.7396
5.87E-01	0.0020	**1.13E+04**	0.7432
7.15E-01	0.0023	**1.37E+04**	0.7461
8.71E-01	0.0028	**1.67E+04**	0.7486
1.06E+00	0.0034	**2.04E+04**	0.7506
1.29E+00	0.0040	**2.48E+04**	0.7523
1.57E+00	0.0049	**3.02E+04**	0.7536

Aptamer 5’-/5Bioseg/-GGG GTT GGG GTG TGG GGT TGG GG-3’ +

Ovalbumin

Table 12 Values collected from UV-Vis measurement during the ELISA procedure for the calculation of the K_d for the aptamer and ovalbumin.

Aptamer Concentration	Absorbance Replicates			Average	SD
	1	2	3		
0	0	0.003	0.004	0.0023	0.0021
0.01	0.001	0.003	0.002	0.0020	0.0010
0.1	0.002	0.002	0.002	0.0020	0.0000
0.5	0.002	0.002	0.002	0.0020	0.0000
1	0.003	0.002	0.001	0.0020	0.0010
5	0.004	0.002	0.002	0.0027	0.0012
10	0.006	0.006	0.002	0.0047	0.0023
50	0.022	0.027	0.027	0.0253	0.0029
100	0.038	0.034	0.034	0.0353	0.0023
1000	0.238	0.255	0.235	0.2427	0.0108
5000	0.413	0.456	0.388	0.4190	0.0344
10000	0.502	0.457	0.441	0.4667	0.0316
20000	0.502	0.534	0.451	0.4957	0.0419
30000	0.485	0.498	0.514	0.4990	0.0145
K_d	1200	1100	1280	1190 nM	90.185
Bmax	0.527	0.531	0.499	0.5190	0.0174

Table 13 Calculated values using Equation 3 for the curve fit for the aptamer with ovalbumin, from Figure 21.

Fit			
Assumed Aptamer Concertation	**Absorbance**	**Assumed Aptamer Concentration**	**Absorbance**
1.00E-04	4.265E-08	**1.92E+00**	0.0008
1.22E-04	5.203E-08	**2.34E+00**	0.0010
1.48E-04	6.311E-08	**2.85E+00**	0.0012
1.81E-04	7.719E-08	**3.47E+00**	0.0015
2.20E-04	9.382E-08	**4.22E+00**	0.0018
2.68E-04	1.143E-07	**5.14E+00**	0.0022
3.27E-04	1.394E-07	**6.26E+00**	0.0027
3.98E-04	1.697E-07	**7.63E+00**	0.0032
4.84E-04	2.064E-07	**9.29E+00**	0.0039
5.90E-04	2.516E-07	**1.13E+01**	0.0048
7.19E-04	3.066E-07	**1.38E+01**	0.0058
8.75E-04	3.731E-07	**1.68E+01**	0.0071
1.07E-03	4.563E-07	**2.05E+01**	0.0086
1.30E-03	5.544E-07	**2.49E+01**	0.0104
1.58E-03	6.738E-07	**3.03E+01**	0.0126
1.93E-03	8.231E-07	**3.70E+01**	0.0153
2.35E-03	1.002E-06	**4.50E+01**	0.0185
2.86E-03	1.220E-06	**5.48E+01**	0.0224
3.48E-03	1.484E-06	**6.68E+01**	0.0270
4.24E-03	1.808E-06	**8.13E+01**	0.0325
5.17E-03	2.205E-06	**9.91E+01**	0.0391
6.29E-03	2.682E-06	**1.21E+02**	0.0470
7.66E-03	3.267E-06	**1.47E+02**	0.0560
9.33E-03	3.979E-06	**1.79E+02**	0.0667
1.14E-02	4.862E-06	**2.18E+02**	0.0791
1.38E-02	5.885E-06	**2.66E+02**	0.0934
1.69E-02	7.207E-06	**3.24E+02**	0.1095
2.05E-02	8.742E-06	**3.94E+02**	0.1275
2.50E-02	1.066E-05	**4.80E+02**	0.1476
3.05E-02	1.301E-05	**5.85E+02**	0.1695
3.71E-02	1.582E-05	**7.12E+02**	0.1929
4.52E-02	1.927E-05	**8.67E+02**	0.2176
5.51E-02	2.350E-05	**1.06E+03**	0.2437
6.71E-02	2.861E-05	**1.29E+03**	0.2696
8.17E-02	3.484E-05	**1.57E+03**	0.2955

9.95E-02	4.243E-05	**1.91E+03**	0.3206
1.21E-01	5.160E-05	**2.33E+03**	0.3451
1.48E-01	6.311E-05	**2.83E+03**	0.3677
1.80E-01	7.675E-05	**3.45E+03**	0.3890
2.19E-01	9.338E-05	**4.20E+03**	0.4083
2.67E-01	0.0001	**5.12E+03**	0.4257
3.25E-01	0.0001	**6.23E+03**	0.4410
3.96E-01	0.0002	**7.59E+03**	0.4545
4.82E-01	0.0002	**9.25E+03**	0.4663
5.87E-01	0.0003	**1.13E+04**	0.4765
7.15E-01	0.0003	**1.37E+04**	0.4849
8.71E-01	0.0004	**1.67E+04**	0.4922
1.06E+00	0.0005	**2.04E+04**	0.4985
1.29E+00	0.0005	**2.48E+04**	0.5036
1.57E+00	0.0007	**3.02E+04**	0.5079

5’- /5Biosg/ GGG GTT GGG GTG TGG GGT TGG GG/3AmMO/
C12 Spacer ssDNA-amphiphile

Table 14 Values collected from UV-Vis measurement during the ELISA procedure for the calculation of the K_d for the C12 ssDNA-amphiphile.

Aptamer Concentration	Absorbance Replicates			Average	SD
	1	2	3		
0	0.03	0.029	0.031	0.030	0.001
0.01	0.036	0.028	0.038	0.034	0.005
0.1	0.034	0.04	0.04	0.038	0.003
0.5	0.051	0.051	0.055	0.052	0.002
1	0.059	0.057	0.059	0.058	0.001
5	0.071	0.075	0.072	0.073	0.002
10	0.097	0.133	0.109	0.113	0.018
50	0.393	0.388	0.444	0.408	0.031
100	0.653	0.652	0.668	0.658	0.009
1000	1.263	1.304	1.308	1.292	0.025
5000	1.458	1.412	1.395	1.422	0.033
10000	1.42	1.45	1.43	1.433	0.015
20000	1.446	1.457	1.449	1.451	0.006
30000	1.464	1.461	1.487	1.471	0.014
K_d	140	137	125	134 nM	7.937
Bmax	1.43	1.44	1.43	1.430	0.006

Table 15 Calculated values using Equation 3 for the curve fit C12 ssDNA-amphiphile, from Figure 22.

Fit			
Assumed Aptamer Concertation	**Absorbance**	**Assumed Aptamer Concentration**	**Absorbance**
1.00E-04	0.0004	**1.92E+00**	0.0229
1.22E-04	0.0004	**2.34E+00**	0.0277
1.48E-04	0.0004	**2.85E+00**	0.0336
1.81E-04	0.0004	**3.47E+00**	0.0406
2.20E-04	0.0004	**4.22E+00**	0.0490
2.68E-04	0.0004	**5.14E+00**	0.0592
3.27E-04	0.0004	**6.26E+00**	0.0714
3.98E-04	0.0004	**7.63E+00**	0.0861
4.84E-04	0.0004	**9.29E+00**	0.1034
5.90E-04	0.0004	**1.13E+01**	0.1239
7.19E-04	0.0004	**1.38E+01**	0.1485
8.75E-04	0.0004	**1.68E+01**	0.1769
1.07E-03	0.0004	**2.05E+01**	0.2103
1.30E-03	0.0004	**2.49E+01**	0.2478
1.58E-03	0.0004	**3.03E+01**	0.2910
1.93E-03	0.0004	**3.70E+01**	0.3406
2.35E-03	0.0004	**4.50E+01**	0.3947
2.86E-03	0.0004	**5.48E+01**	0.4544
3.48E-03	0.0004	**6.68E+01**	0.5192
4.24E-03	0.0004	**8.13E+01**	0.5874
5.17E-03	0.0004	**9.91E+01**	0.6591
6.29E-03	0.0005	**1.21E+02**	0.7331
7.66E-03	0.0005	**1.47E+02**	0.8054
9.33E-03	0.0005	**1.79E+02**	0.8775
1.14E-02	0.0005	**2.18E+02**	0.9471
1.38E-02	0.0005	**2.66E+02**	1.0138
1.69E-02	0.0006	**3.24E+02**	1.0753
2.05E-02	0.0006	**3.94E+02**	1.1312
2.50E-02	0.0007	**4.80E+02**	1.1822
3.05E-02	0.0007	**5.85E+02**	1.2277
3.71E-02	0.0008	**7.12E+02**	1.2675
4.52E-02	0.0009	**8.67E+02**	1.3023
5.51E-02	0.0010	**1.06E+03**	1.3329
6.71E-02	0.0012	**1.29E+03**	1.3584
8.17E-02	0.0013	**1.57E+03**	1.3801

9.95E-02	0.0016	**1.91E+03**	1.3985
1.21E-01	0.0018	**2.33E+03**	1.4142
1.48E-01	0.0021	**2.83E+03**	1.4270
1.80E-01	0.0025	**3.45E+03**	1.4379
2.19E-01	0.0030	**4.20E+03**	1.4469
2.67E-01	0.0036	**5.12E+03**	1.4545
3.25E-01	0.0042	**6.23E+03**	1.4607
3.96E-01	0.0051	**7.59E+03**	1.4659
4.82E-01	0.0061	**9.25E+03**	1.4701
5.87E-01	0.0073	**1.13E+04**	1.4737
7.15E-01	0.0088	**1.37E+04**	1.4765
8.71E-01	0.0107	**1.67E+04**	1.4789
1.06E+00	0.0129	**2.04E+04**	1.4809
1.29E+00	0.0156	**2.48E+04**	1.4825
1.57E+00	0.0189	**3.02E+04**	1.4839

5’- /5Biosg/ GGG GTT GGG GTG TGG GGT TGG GG/3AmMO/
T10 Spacer ssDNA-amphiphile

Table 16 Values collected from UV-Vis measurement during the ELISA procedure for the calculation of the K_d for the T10 ssDNA-amphiphile.

Aptamer Concentration	Absorbance Replicates			Average	SD
	1	2	3		
0	0.053	0.053	0.041	0.0490	0.0069
0.01	0.05	0.051	0.051	0.0507	0.0006
0.1	0.055	0.058	0.055	0.0560	0.0017
0.5	0.068	0.061	0.058	0.0623	0.0051
1	0.072	0.075	0.069	0.0720	0.0030
5	0.068	0.084	0.079	0.0770	0.0082
10	0.093	0.099	0.091	0.0943	0.0042
50	0.477	0.473	0.471	0.4737	0.0031
100	0.65	0.657	0.659	0.6553	0.0047
1000	1.214	1.306	1.242	1.2540	0.0472
5000	1.455	1.371	1.372	1.3993	0.0482
10000	1.417	1.438	1.431	1.4287	0.0107
20000	1.398	1.466	1.404	1.4227	0.0376
30000	1.427	1.438	1.408	1.4243	0.0152
K_d	131	128	122	127nM	4.5826
Bmax	1.38	1.4	1.37	1.3800	0.0153

Table 17 Calculated values using Equation 3 for the curve fit T10 ssDNA-amphiphile, from Figure 23.

Fit			
Assumed Aptamer Concertation	**Absorbance**	**Assumed Aptamer Concentration**	**Absorbance**
1.00E-04	0.0004	**1.92E+00**	0.0227
1.22E-04	0.0004	**2.34E+00**	0.0274
1.48E-04	0.0004	**2.85E+00**	0.0332
1.81E-04	0.0004	**3.47E+00**	0.0401
2.20E-04	0.0004	**4.22E+00**	0.0484
2.68E-04	0.0004	**5.14E+00**	0.0585
3.27E-04	0.0004	**6.26E+00**	0.0705
3.98E-04	0.0004	**7.63E+00**	0.0850
4.84E-04	0.0004	**9.29E+00**	0.1021
5.90E-04	0.0004	**1.13E+01**	0.1223
7.19E-04	0.0004	**1.38E+01**	0.1466
8.75E-04	0.0004	**1.68E+01**	0.1746
1.07E-03	0.0004	**2.05E+01**	0.2075
1.30E-03	0.0004	**2.49E+01**	0.2445
1.58E-03	0.0004	**3.03E+01**	0.2870
1.93E-03	0.0004	**3.70E+01**	0.3358
2.35E-03	0.0004	**4.50E+01**	0.3890
2.86E-03	0.0004	**5.48E+01**	0.4477
3.48E-03	0.0004	**6.68E+01**	0.5114
4.24E-03	0.0004	**8.13E+01**	0.5784
5.17E-03	0.0005	**9.91E+01**	0.6487
6.29E-03	0.0005	**1.21E+02**	0.7213
7.66E-03	0.0005	**1.47E+02**	0.7921
9.33E-03	0.0005	**1.79E+02**	0.8627
1.14E-02	0.0005	**2.18E+02**	0.9308
1.38E-02	0.0006	**2.66E+02**	0.9959
1.69E-02	0.0006	**3.24E+02**	1.0560
2.05E-02	0.0006	**3.94E+02**	1.1106
2.50E-02	0.0007	**4.80E+02**	1.1603
3.05E-02	0.0008	**5.85E+02**	1.2047
3.71E-02	0.0008	**7.12E+02**	1.2435
4.52E-02	0.0009	**8.67E+02**	1.2774
5.51E-02	0.0010	**1.06E+03**	1.3071
6.71E-02	0.0012	**1.29E+03**	1.3320
8.17E-02	0.0014	**1.57E+03**	1.3532

9.95E-02	0.0016	**1.91E+03**	1.3710
1.21E-01	0.0018	**2.33E+03**	1.3862
1.48E-01	0.0021	**2.83E+03**	1.3987
1.80E-01	0.0025	**3.45E+03**	1.4094
2.19E-01	0.0030	**4.20E+03**	1.4181
2.67E-01	0.0035	**5.12E+03**	1.4255
3.25E-01	0.0042	**6.23E+03**	1.4315
3.96E-01	0.0050	**7.59E+03**	1.4365
4.82E-01	0.0060	**9.25E+03**	1.4407
5.87E-01	0.0073	**1.13E+04**	1.4442
7.15E-01	0.0088	**1.37E+04**	1.4469
8.71E-01	0.0106	**1.67E+04**	1.4492
1.06E+00	0.0128	**2.04E+04**	1.4512
1.29E+00	0.0154	**2.48E+04**	1.4527
1.57E+00	0.0186	**3.02E+04**	1.4540

5’- /5Biosg/ GGG GTT GGG GTG TGG GGT TGG GG/3AmMO/
No Spacer ssDNA-amphiphile

Table 18 Values collected from UV-Vis measurement during the ELISA procedure for the calculation of the K_d for the No Spacer ssDNA-amphiphile.

Aptamer Concentration	Absorbance Replicates			Average	SD
	1	2	3		
0	0.068	0.068	0.059	0.0650	0.0052
0.01	0.072	0.071	0.065	0.0693	0.0038
0.1	0.073	0.072	0.069	0.0713	0.0021
0.5	0.096	0.087	0.074	0.0857	0.0111
1	0.106	0.097	0.084	0.0957	0.0111
5	0.105	0.103	0.108	0.1053	0.0025
10	0.415	0.448	0.409	0.4240	0.0210
50	1.509	1.474	1.486	1.4896	0.0177
100	1.829	1.918	1.837	1.8613	0.0492
1000	2.53	2.52	2.465	2.5050	0.0350
5000	2.555	2.555	2.6	2.5700	0.0260
10000	2.541	2.552	2.606	2.5663	0.0348
20000	2.563	2.524	2.624	2.5703	0.0504
30000	2.597	2.55	2.553	2.5667	0.0263
K_d	45.4	43.2	46.5	45 nM	1.6803
Bmax	2.53	2.51	2.55	2.5300	0.0200

Table 19 Calculated values using Equation 3 for the curve fit No Spacer ssDNA-amphiphile, from Figure 24.

Fit			
Assumed Aptamer Concertation	**Absorbance**	**Assumed Aptamer Concentration**	**Absorbance**
1.00E-04	0.0014	**1.92E+00**	0.1047
1.22E-04	0.0014	**2.34E+00**	0.1262
1.48E-04	0.0014	**2.85E+00**	0.1517
1.81E-04	0.0015	**3.47E+00**	0.1821
2.20E-04	0.0015	**4.22E+00**	0.2178
2.68E-04	0.0015	**5.14E+00**	0.2601
3.27E-04	0.0015	**6.26E+00**	0.3096
3.98E-04	0.0015	**7.63E+00**	0.3673
4.84E-04	0.0015	**9.29E+00**	0.4333
5.90E-04	0.0015	**1.13E+01**	0.5080
7.19E-04	0.0015	**1.38E+01**	0.5939
8.75E-04	0.0015	**1.68E+01**	0.6877
1.07E-03	0.0015	**2.05E+01**	0.7916
1.30E-03	0.0015	**2.49E+01**	0.9009
1.58E-03	0.0015	**3.03E+01**	1.0176
1.93E-03	0.0015	**3.70E+01**	1.1410
2.35E-03	0.0016	**4.50E+01**	1.2643
2.86E-03	0.0016	**5.48E+01**	1.3885
3.48E-03	0.0016	**6.68E+01**	1.5109
4.24E-03	0.0017	**8.13E+01**	1.6278
5.17E-03	0.0017	**9.91E+01**	1.7392
6.29E-03	0.0018	**1.21E+02**	1.8434
7.66E-03	0.0019	**1.47E+02**	1.9364
9.33E-03	0.0020	**1.79E+02**	2.0211
1.14E-02	0.0021	**2.18E+02**	2.0966
1.38E-02	0.0022	**2.66E+02**	2.1634
1.69E-02	0.0024	**3.24E+02**	2.2210
2.05E-02	0.0026	**3.94E+02**	2.2703
2.50E-02	0.0028	**4.80E+02**	2.3128
3.05E-02	0.0032	**5.85E+02**	2.3490
3.71E-02	0.0035	**7.12E+02**	2.3794
4.52E-02	0.0040	**8.67E+02**	2.4050
5.51E-02	0.0045	**1.06E+03**	2.4268
6.71E-02	0.0052	**1.29E+03**	2.4446
8.17E-02	0.0060	**1.57E+03**	2.4594

9.95E-02	0.0070	**1.91E+03**	2.4717
1.21E-01	0.0082	**2.33E+03**	2.4820
1.48E-01	0.0097	**2.83E+03**	2.4903
1.80E-01	0.0115	**3.45E+03**	2.4974
2.19E-01	0.0137	**4.20E+03**	2.5031
2.67E-01	0.0163	**5.12E+03**	2.5079
3.25E-01	0.0195	**6.23E+03**	2.5118
3.96E-01	0.0234	**7.59E+03**	2.5151
4.82E-01	0.0282	**9.25E+03**	2.5177
5.87E-01	0.0339	**1.13E+04**	2.5199
7.15E-01	0.0409	**1.37E+04**	2.5217
8.71E-01	0.0493	**1.67E+04**	2.5232
1.06E+00	0.0595	**2.04E+04**	2.5244
1.29E+00	0.0718	**2.48E+04**	2.5254
1.57E+00	0.0865	**3.02E+04**	2.5262

Appendix C- Results of the preliminary surface swab test.

For the swab test three surfaces were selected, Table 20. Squares of 4 in side were used as the reference for the test.

Table 20 Food Contact surfaces used for the swab test.

HDPE	Stainless Steel	Ceramic Tile
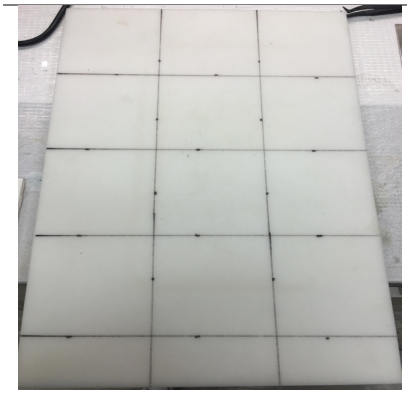	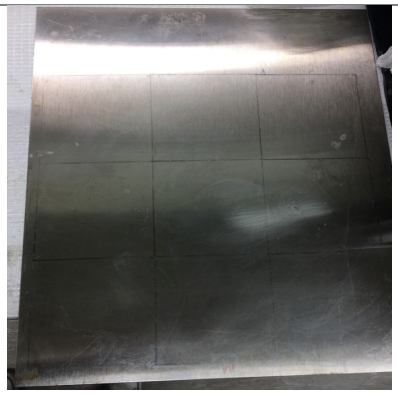	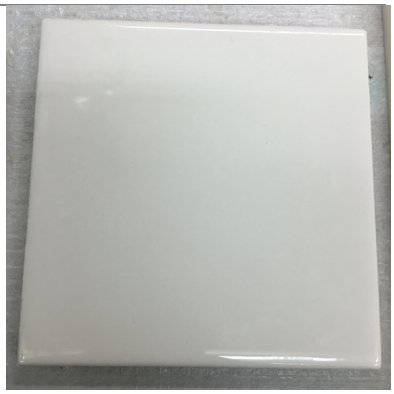

The result for this test can be seen on the Figure below.

HDPE	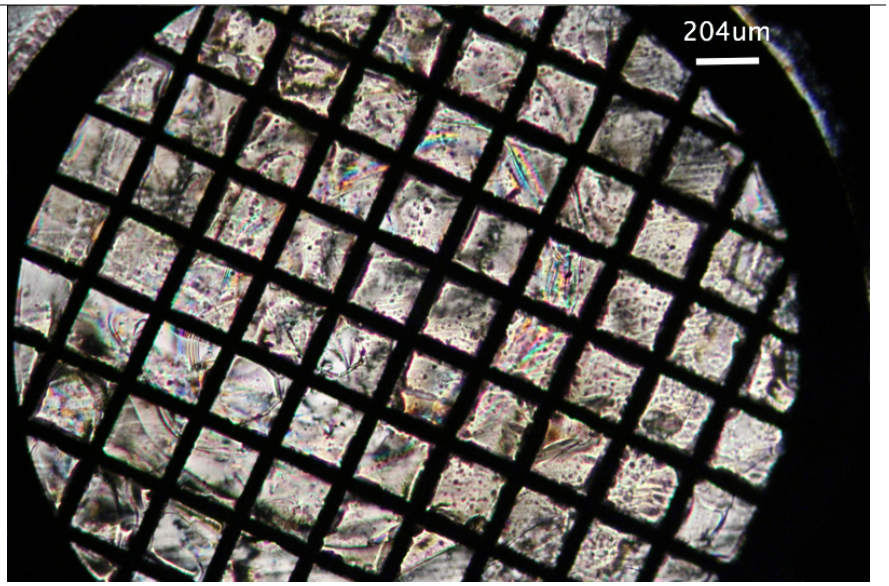
Stainless Steel	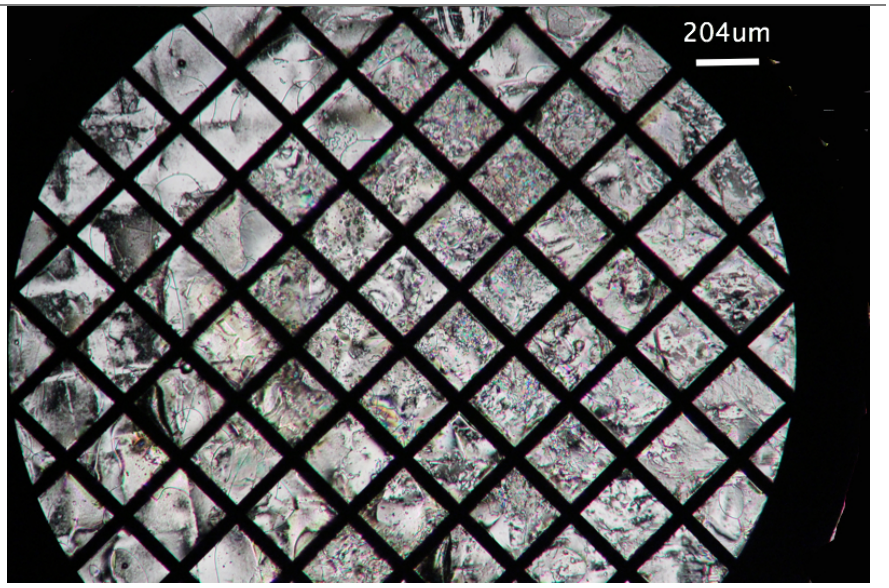

Tile	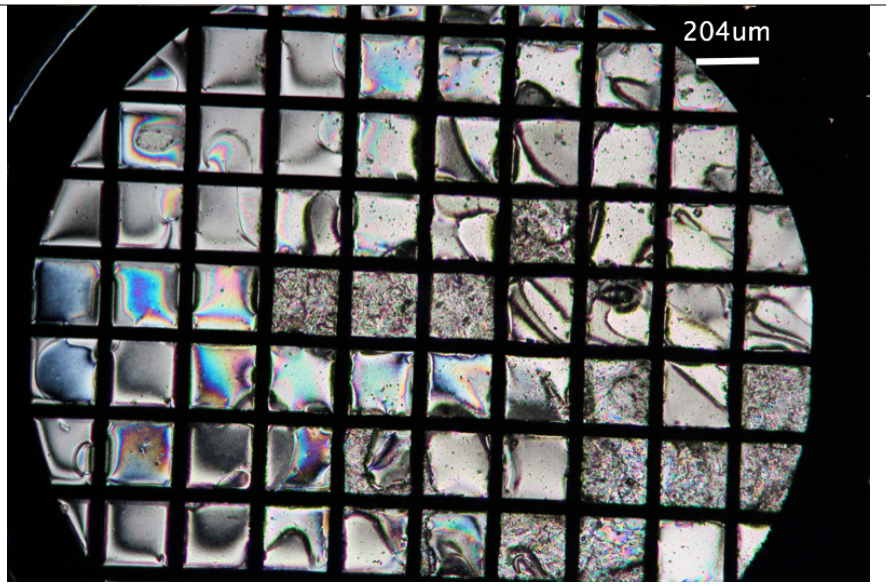
Water	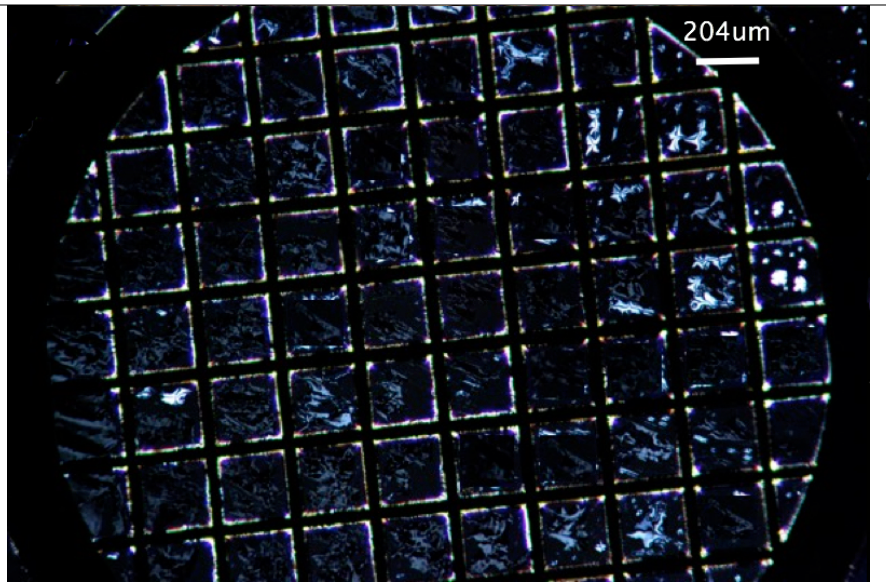

Figure 37 Optical images of the 5CB LC confined to a copper grid supported on a OTS treated glass under the polarizing microscope. The images reflect the LC exposed to the aptamer-amphiphile and subsequently to the solution from the swab test. The images were obtained using a Nikon microscope with transmitted polarized lights and a digital Canon camera

As showed in Figure 37, the swab test was able to collect protein from the surface of steal, HDPE, and ceramic tile and the images obtained were as it was expected. Bright images were obtained when protein solution was used for the test and a dark image was obtained when water was used. This result demonstrates that this sensor can be potentially used as a surface test for processing plants to try to avoid cross-contact problems and to ensure a truthful product label.